Hybrid Particle-Continuum Numerical Methods for Aerospace Applications

Iain D. Boyd and Timothy R. Deschenes
Department of Aerospace Engineering
University of Michigan
Ann Arbor, Michigan, USA

iainboyd@umich.edu

Abstract

Often, rarefied flows of interest in aerospace applications are embedded within largely continuum flow fields. Neither continuum nor kinetic methods provide both physically accurate and numerically efficient techniques to simulate the entire flow field. Instead, multi-scale methods can provide the capability of achieving the efficiency of continuum methods in regions where the degree of collisional nonequilibrium is small, while maintaining the physical accuracy of kinetic methods in rarefied portions of the flow. This work begins with an outline of typical aerospace flows that may require a multi-scale analysis in order to make accurate and efficient predictions. It then provides an overview of the research performed in developing hybrid methods for partially rarefied gas flows. Finally, some results derived from current state of the art hybrid codes are presented and emerging developments are described.

1 Introduction

Typically, the Knudsen number, shown in Eq. 1, which is the ratio of the mean free path, λ, to a characteristic length scale, L, is used to determine the degree of collisional nonequilibrium in a gas flow.

$$Kn = \frac{\lambda}{L} \tag{1}$$

When Kn is large, very few molecular collisions occur, and the entire flow is considered to be in collisional nonequilibrium, or rarefied. For rarefied flows, the direct simulation Monte Carlo (DSMC) method [1] can

Report Documentation Page

Form Approved
OMB No. 0704-0188

1. REPORT DATE	2. REPORT TYPE	3. DATES COVERED
JAN 2011	**N/A**	**-**

4. TITLE AND SUBTITLE	5a. CONTRACT NUMBER
Hybrid Particle-Continuum Numerical Methods for Aerospace Applications	5b. GRANT NUMBER
	5c. PROGRAM ELEMENT NUMBER
6. AUTHOR(S)	5d. PROJECT NUMBER
	5e. TASK NUMBER
	5f. WORK UNIT NUMBER
7. PERFORMING ORGANIZATION NAME(S) AND ADDRESS(ES) **Department of Aerospace Engineering University of Michigan Ann Arbor, Michigan, USA**	8. PERFORMING ORGANIZATION REPORT NUMBER
9. SPONSORING/MONITORING AGENCY NAME(S) AND ADDRESS(ES)	10. SPONSOR/MONITOR'S ACRONYM(S)
	11. SPONSOR/MONITOR'S REPORT NUMBER(S)

12. DISTRIBUTION/AVAILABILITY STATEMENT
Approved for public release, distribution unlimited

13. SUPPLEMENTARY NOTES
See also ADA579248. Models and Computational Methods for Rarefied Flows (Modeles et methodes de calcul des coulements de gaz rarefies). RTO-EN-AVT-194

14. ABSTRACT
Often, rareed ows of interest in aerospace applications are embedded within largely continuum ow elds. Neither continuum nor kinetic methods provide both physically accurate and numerically ecient techniques to simulate the entire ow eld. Instead, multi-scale methods can provide the capability of achieving the eciency of continuum methods in regions where the degree of collisional nonequilibrium is small, while maintaining the physical accuracy of kinetic methods in rareed portions of the ow. This work begins with an outline of typical aerospace ows that may require a multi-scale analysis in order to make accurate and ecient predictions. It then provides an overview of the research performed in developing hybrid methods for partially rareed gas ows. Finally, some results derived from current state of the art hybrid codes are presented and emerging developments are described.

15. SUBJECT TERMS

16. SECURITY CLASSIFICATION OF:			17. LIMITATION OF ABSTRACT	18. NUMBER OF PAGES	19a. NAME OF RESPONSIBLE PERSON
a. REPORT **unclassified**	b. ABSTRACT **unclassified**	c. THIS PAGE **unclassified**	**SAR**	**36**	

provide an efficient and physically accurate prediction, however the numerical expense of DSMC increases as the Knudsen number decreases. If $Kn \ll 1$, the flow can be considered approximately in collisional equilibrium, or continuum, and a numerical solution of the Navier-Stokes equations with modern computational fluid dynamics (CFD) can be found efficiently with very little loss in physical accuracy. However, the physical accuracy of the continuum, Navier-Stokes equations degrades as the Knudsen number increases.

For many cases, the characteristic length scale and/or mean free path may vary significantly throughout the flow field, especially when the flow is in the transitional regime between fully rarefied or continuum. In these multi-scale flows, some regions may have large characteristic length scales compared to the local mean free path such that they are entirely within the continuum domain and efficient prediction with kinetic methods, such as DSMC, is not possible. These same flows may contain regions where the characteristic length scales are very small compared to the local mean free path, such that the physical accuracy of continuum methods breaks down. Although there are techniques that extend the continuum formulation by use of slip boundary conditions, they often do not fill the entire gap of applicability between continuum and rarefied simulation techniques. Therefore, application of either continuum or rarefied simulation methods to the entire domain of flow fields in the transition regime can not maintain both physical accuracy and numerical efficiency.

Alternatively, a multi-scale, hybrid method can be applied to these flows. Such a method uses a continuum solver in regions that are very near collisional equilibrium, while using rarefied gas simulation methods in regions that exhibit continuum breakdown. In this work, we use the definition of a hybrid particle-continuum method proposed by Wilmoth et al. [2] as an algorithm that performs two-way information exchange between particle and continuum simulation methods.

The proceeding section will outline examples of multi-scale flows to which hybrid particle-continuum methods can be applied. Next, Sec. 3 outlines the research that has been performed specific to developing hybrid particle-continuum methods. Section 4 gives an overview of the published hybrid particle-continuum algorithms and a selection of results demonstrated from each proposed method. Finally, Sec. 5 provides a summary of the paper and an outline of some future challenges that still exist to extend the current state of the art in hybrid particle-continuum simulation techniques.

2 Examples of Multi-Scale Flows in Aerospace Applications

Flows in the transitional regime have small length scales due to the geometry or flow structure. For example, the geometric size of MEMS devices is sufficiently small that the molecular nature of the gas is important and a kinetic treatment may be required in some regions of the flow to maintain physical accuracy. Conversely, hypersonic vehicles flying in the upper atmosphere experience flow with a large mean free path due to the relatively low atmospheric density. In addition, these hypersonic vehicles create high gradient flow features, such as strong shocks, strong expansions, and thin boundary layers that exhibit very small flow length scales. A hybrid particle-continuum method is well suited to simulate internal or external flows that exhibit a large variation of characteristic flow and/or collision length scales. This subsection will outline some typical flows that can exhibit these flow features and may be suited for application of a hybrid particle-continuum method.

2.1 Micro-Scale Flows

Recently, an increase in the development of micro- and nano-electromechanical systems (MEMS/NEMS) has occurred due to the low costs associated with batch-manufacturing, low energy requirements, and small size. Many applications of MEMS/NEMS devices, which include micro-turbines [3, 4], micro-sensors for chemical concentrations or gas flow properties [5, 6, 7, 8], and spacecraft micro-propulsion [9], involve gas flows. However, the general understanding of micro-scale gas flows lags behind the fabrication and application of these MEMS/NEMS devices. Experiments have shown that the fluid mechanics of micro-scale gas flows are not the same as those experienced in similar, larger-scaled devices. For example, the pressure distribution in a long micro-channel has been observed to be nonlinear [10], and the measured flow rate in a micro-channel was higher than predicted using the Navier-Stokes equations [11]. Although the use of slip boundary conditions within a Navier-Stokes solver has provided some improvement over application of the no-slip boundary condition, this can only provide a small extension of application of the Navier-Stokes equations in the near continuum regime. Instead, application of a hybrid method that uses a physically accurate particle method in all regions where the Navier-Stokes equations are invalid (rather than just at the surface) can provide reliable predictions throughout the rarefied-continuum flow regime.

2.2 Hypersonic, Blunt-Body Flows

At moderately high altitudes, some regions of the flow about blunted, hypersonic vehicles can be rarefied due to very small length scales, within a mostly continuum flow field. For example, Fig. 1 shows a Schlieren image of typical flow over a blunted, hypersonic vehicle. In general, the flow length scales within the thin bow shock and boundary layer are small and the collision length scales in the wake are sufficiently large such that a microscopic analysis of these regions is required to maintain the physical accuracy of the simulation. As the vehicle spends a larger portion of its time in these partially-rarefied flows with recently proposed trajectory maneuvers [12], the ability to maintain physically accurate predictions becomes even more important to minimize the predictive uncertainty and increase vehicle reliability. Recently, a skip trajectory, where an entry vehicle "skips" through the upper atmosphere as illustrated in Fig. 3, has been proposed to increase the downrange capabilities and reduce peak heating of hypersonic entry vehicles.

The AS-202 flight case from the Apollo program is one of the few flight tests that used a skip trajectory. Wright et al. [14] performed detailed simulations of the entire flight trajectory using a continuum description of the flow. In general, they found that agreement between available heat transfer measurements from the flight tests and numerical predictions was good over most of the trajectory. However, at the crest of the skip portion of the trajectory, the simulation results over-predict the measured data across most of the lee side of the aft-body. For example, Fig. 2 compares heat transfer predictions and flight measurements from a calorimeter located on the top of the lee side. During the skip portion, the CFD simulation method over-predict the measurements by over a factor of two. Based on the reconstructed data shown in Fig. 3 and the corresponding Knudsen number at this altitude shown in Fig. 4, it is possible that the vehicle has transitioned from being fully continuum to partially rarefied as the vehicle has passed from the trough to the crest of the skip portion of the trajectory. Because of this, Wright et al. concluded that the over-prediction of heat transfer may be due to the inability of the continuum methods used in that work to capture the important microscopic effects. However, for this

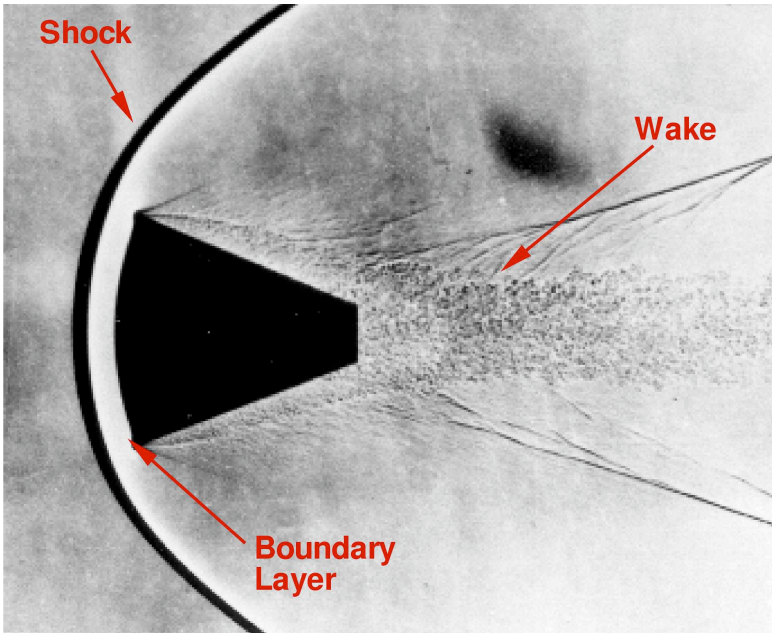

Figure 1: Schematic of hypersonic flow over a blunted body with regions that typically exhibit non-continuum effects [13]

particular flow, application of kinetic methods to the entire flow would be computationally expensive. Instead, a multi-scale approach that only uses the expensive, microscopic description in required regions, while using the continuum description throughout the rest of the flow field, is more suitable to examine any rarefied flow effects.

Simulation of other multi-scale, hypersonic flows is of particular importance for developing technologies that will enable potential high-mass, Mars missions. Compared to the Earth's atmosphere, Mars' relatively thin atmosphere causes entry vehicles to decelerate at much lower altitudes. Depending on the mass, size, and shape of a vehicle, it may never reach a subsonic terminal velocity. This necessitates additional technology to slow the vehicle so that it can reach subsonic speeds with sufficient time to prepare for landing. Many of these new technologies require successful prediction of multi-scale interaction flows to ensure reliability. In order to increase the frontal area of the vehicle, an inflatable aerodynamic decelerator (IAD) (examples shown in Fig. 6), often called a ballute, may be used to slow the vehicle down at higher altitudes [15]. The dynamic fluid structure interaction at deployment will most certainly occur in the rarefied regime [16] and will require a detailed fluid structure interaction with accurate prediction of surface properties throughout the entire trajectory. In addition, the flow field around the deployed ballute in the upper atmosphere will include both large regions of continuum flow, due to the very large body, and small nonequilibrium interactions around tethers, connections, and the low density wake which may require kinetic analysis. Another possible option that will enable high-mass, Mars missions is supersonic retro-propulsion [17], where a jet is aimed out the front of the aeroshell displacing the shock and increasing the total axial force on the vehicle. At high altitudes, these flows may include a very dense, continuum region within the core of the jet, while much of the flow may be rarefied. For example, Fig. 7 shows the flow around a 70° blunted sphere aeroshell with a propulsive decelerator jet activated at the center-line. The collision length scales within the jet are extremely small, such that the Navier-Stokes equations are valid, and application of kinetic analysis to this region would be computationally intensive. Conversely, the flow length

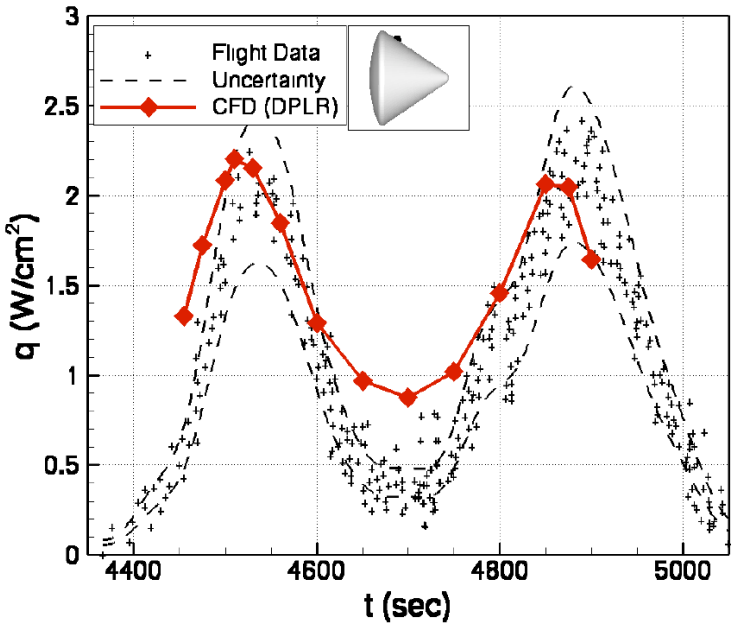

Figure 2: Heat transfer predictions made by macroscopic methods (CFD) on the after-body of the AS-202 flight capsule and comparison with experimental flight data [14]

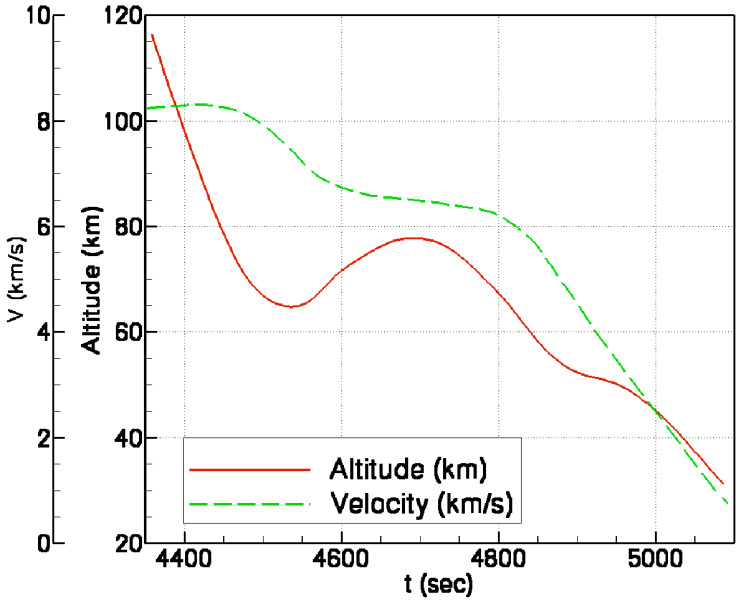

Figure 3: Reconstruction of the AS-202 flight trajectory [14]

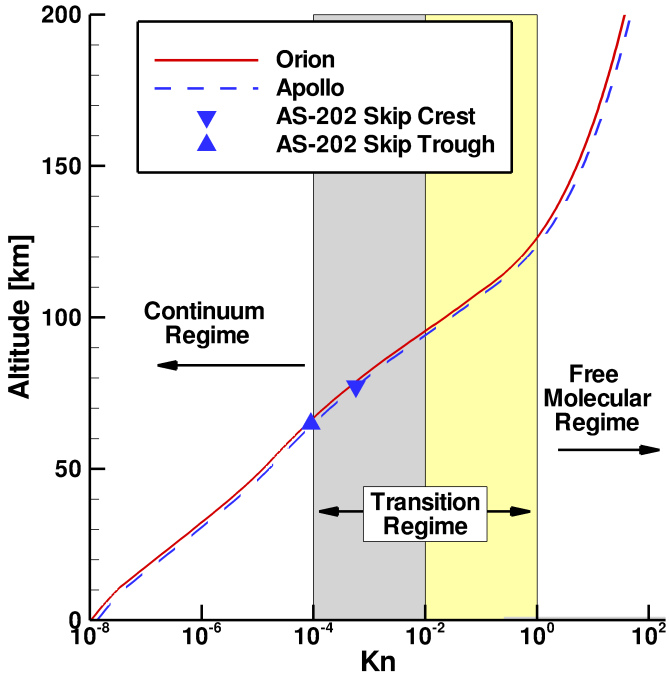

Figure 4: Variation of Knudsen number throughout the Earth's atmosphere for Orion and Apollo capsules

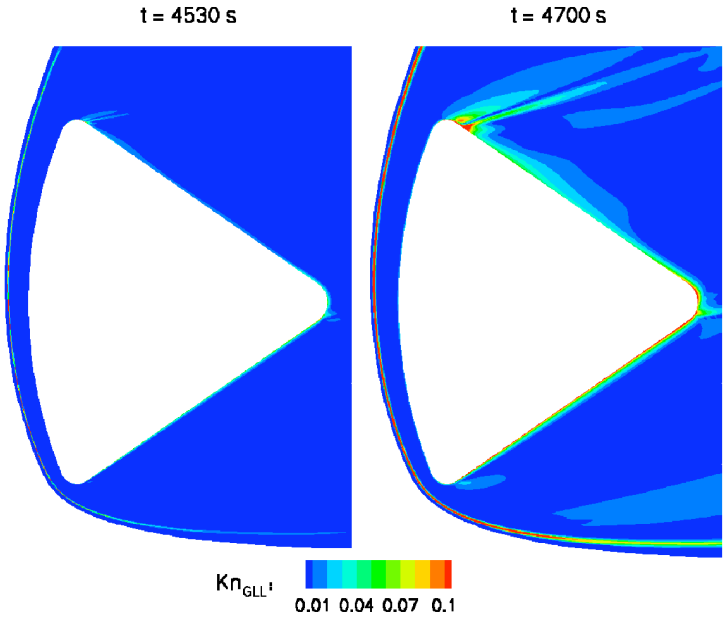

Figure 5: Variation of the gradient-length Knudsen number for flow over the AS-202 capsule at two different trajectory points [14]

Figure 6: Typical Inflatable Aerodynamic Decelerators (IAD) [18]

scales around much of the aeroshell are on the same order of magnitude as the collision length scales, and use of a microscopic method in this region is vital to maintain the necessary physical accuracy. Multi-scale methods that can accurately simulate these flow fields will be an indispensable tool in development of these new technologies that enable future scientific and exploration missions [15].

2.3 Plumes

Another class of multi-scale flows of interest is rocket exhaust plumes. Efficient and accurate predictions of atmospheric exhaust plumes at high altitudes are necessary to ensure that the chemical rocket maintains efficiency while also assuring that the vehicle heating due to the complicated flow structure related to the under-expanded supersonic jet is well understood. For example, Fig. 8 shows the continuum-rarefied interfaces for flow around a sounding rocket traveling in the upper atmosphere. Here, the flow inside the nozzle and the core of the plume are continuum, while the flow around the vehicle and in the outer plume is rarefied. Figure 9 shows the same rocket during a simulated stage separation. Now the flow around the fore-body of the separated stage is entirely continuum, while the external flow is rarefied. Application of full DSMC to these partially rarefied flow fields will require a large computational expense. Instead, application of a multi-scale method will alleviate the cost of resolving flow features in the highly collisional nozzle and jet core regions.

In space flight, knowledge of plume impingement on surfaces is necessary to characterize the interaction with nearby space craft and possible deterioration of solar arrays. In addition, space vehicles landing on dusty asteroids or the Moon can create dust and debris hazards for themselves and other nearby vehicles. Accurate prediction of the nearby flow fields at all thrust conditions is necessary to quantify risk and develop mitigation strategies. For example, Lumpkin et al. [20] performed zonally decoupled DSMC-CFD simulation of the RCS plume impingement of the reaction control systems of the shuttle orbiter during a docking maneuver with the International Space Station. Figure 10 shows a planar slice of the DSMC results with the continuum zones highlighted. This work also included a study of the interaction of the Apollo Lunar Module jet impinging on the lunar surface and the formation of a crater of dust. An illustration of a typical simulation is shown in Fig. 11. Their study results were mixed and found that the decoupled approach may increase the computational cost compared to a coupled approach since the CFD-DSMC interface region had to be placed well into the continuum regime to be upstream of any impingement shock waves. This resulted in DSMC only resolving gross flow features, while finer features,

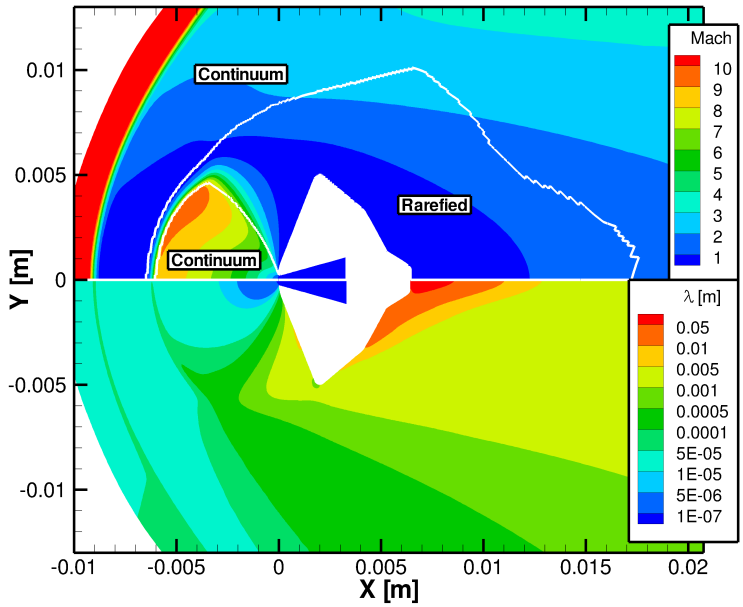

Figure 7: Continuum/rarefied domains for flow over an aeroshell with a propulsive decelerator activated in a partially rarefied flow field with a nominal global Knudsen number of 0.002 based on the aeroshell diameter and free stream Mach number of 12

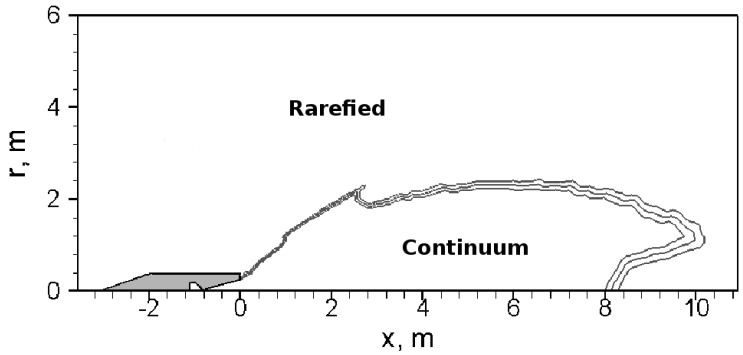

Figure 8: Continuum/rarefied domains for a high altitude rocket plume [19]

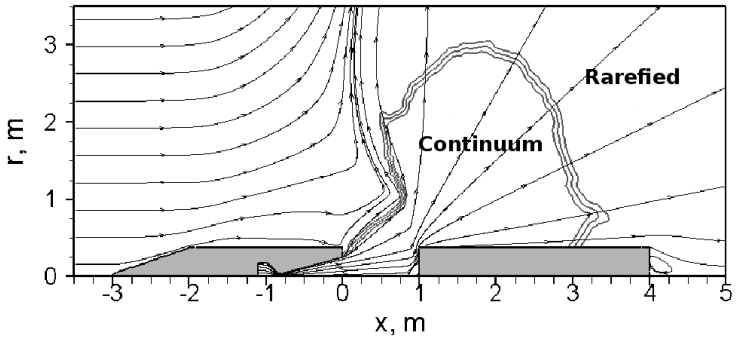

Figure 9: Continuum/rarefied domains for a rocket at stage separation [19]

such as surface shear, have visible, unphysical numerical artifacts. Instead, a fully coupled hybrid method may provide a significant reduction in computational expense, with little loss of physical accuracy.

2.4 Viscous Interaction Flows

Hypersonic viscous interaction flows involve the interactions between shock waves and boundary layers, producing complex and highly non-linear flow fields. Shock-boundary layer interactions occur in inlets of supersonic and hypersonic propulsion devices and in the vicinity of control surfaces on hypersonic vehicles. In such flows, shock-shock interactions often produce reflected shock waves that impinge on the surface of the vehicle. The interaction between a strong shock wave and a boundary layer often causes the flow to separate and form a region of high-pressure, recirculating gas next to the surface. High-speed flow hitting such a separation region significantly alters shock structures and interaction regions which, in turn, affect the extent of flow separation. Peak aerothermal loads are observed at the location of shock impingement on the vehicle surface and therefore accurate prediction of this phenomenon is important in the design of a hypersonic vehicle. In addition, the heating and frictional loads generated within a separated region are drastically different than when the flow is purely attached. Such differences may reduce the effectiveness of a control surface and thus accurately predicting the extent of any flow separation is also a very important aspect in the design of hypersonic vehicles.

An example of a viscous interaction flow is shown in Fig. 12 which was part of a blind validation study with experimental measurements taken in the Large Energy National Shock (LENS) facility at the Calspan - University of Buffalo Research Center (CUBRC) [21]. For Run 11, which had a global Knudsen number of 0.0008, it has been found that solutions to the Navier-Stokes equations predict a separation bubble that forms along the surface that is significantly larger than experimental measurements. In general, DSMC predictions of the same case have better agreement with the experimental measurements in this leading edge region, but require a large computational expense to accurately resolve the shock impingement downstream of the flare junction [21, 22]. Instead, if a multi-scale method can apply a continuum solver in regions where the mean free path is small, and the Navier-Stokes equations are valid, the computational requirements of obtaining a physically accurate solution may be reduced.

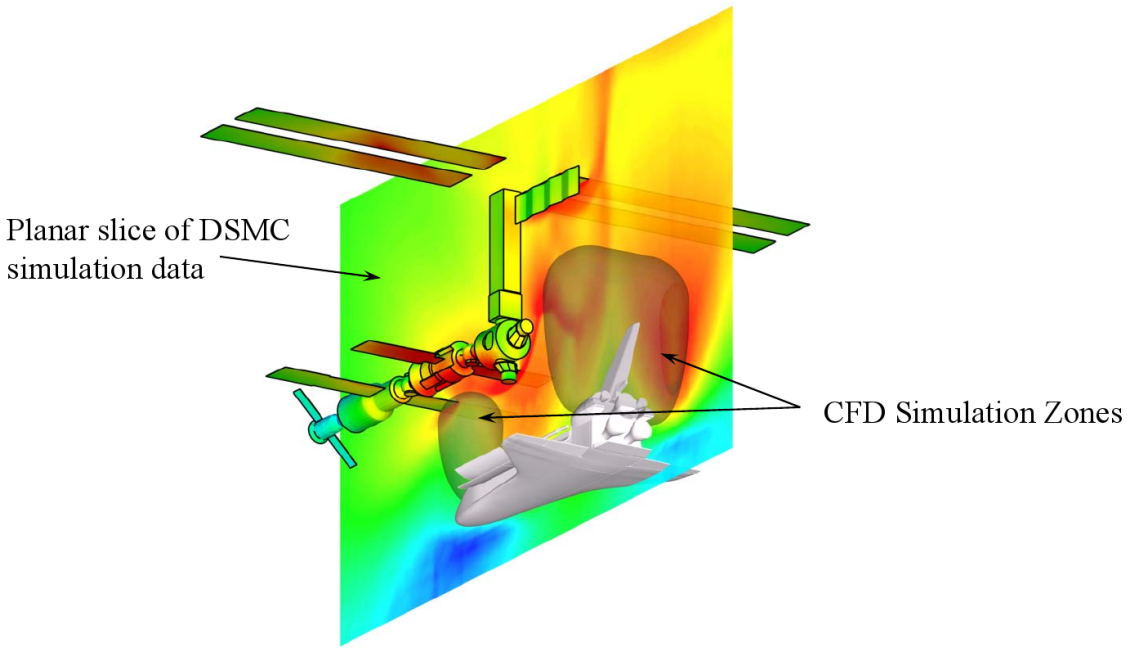

Figure 10: Plume impingement study of the shuttle orbiter docking with the international space station [20]

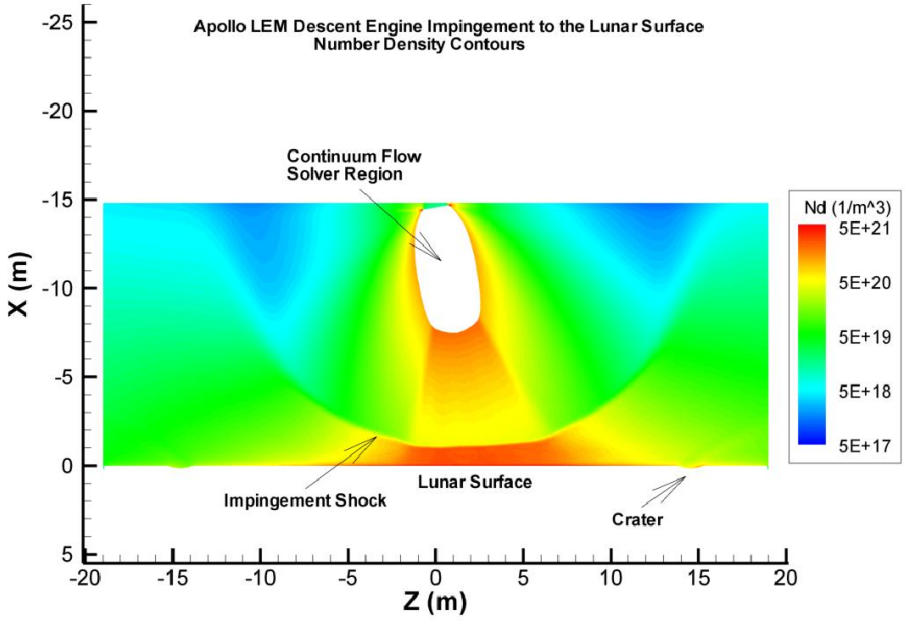

Figure 11: Plume impingement study of the Apollo Lunar Module with the lunar surface [20]

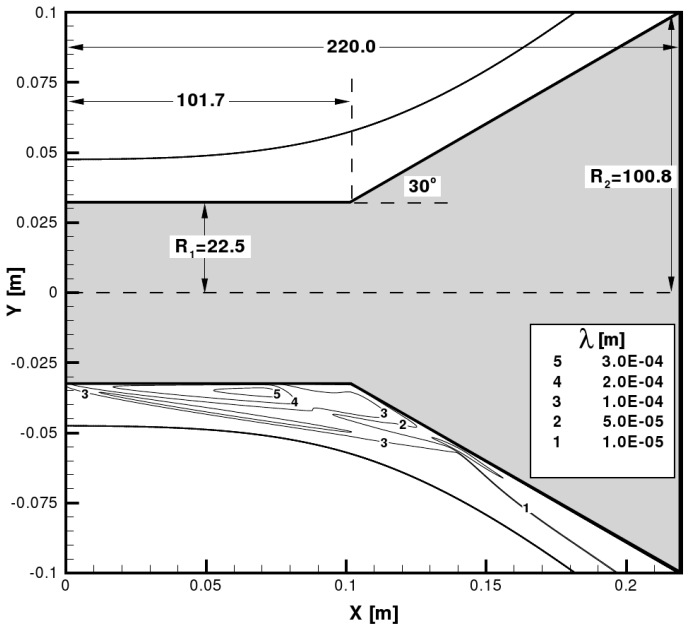

Figure 12: Geometry and variation in mean free path for a hypersonic shock-boundary layer interaction test case [23]

3 Hybrid Particle-Continuum Framework

This section provides an overview of typical challenges associated with the development of hybrid particle-continuum simulation techniques along with published solutions. First, an overview of methods to compute the demarcation between continuum and rarefied regions of the flow is provided. Then, typical coupling procedures used to transfer information between flow modules is outlined.

3.1 Continuum Breakdown

Both the accuracy and efficiency of a hybrid DSMC-CFD method depend strongly on proper placement of the interface location. For physical accuracy, the interface must be located within regions that can be considered in collisional equilibrium, where the velocity distribution is only slightly perturbed from equilibrium, and the Navier-Stokes equations are valid. To maximize efficiency, a hybrid method requires the interface between CFD and DSMC to be located near the edge of the collisional equilibrium region. Empirical breakdown parameters have been used both as switching criteria for hybrid rarefied-continuum methods and also in analysis of continuum predictions to ensure that the Navier-Stokes equations are valid throughout the flow field.

Bird [24] studied DSMC simulations of expansion flows and proposed a continuum breakdown parameter, P, for expansions shown in Eq. 2 where ν is the collision frequency and ρ is the mass density. Through comparison of many one dimensional simulations of spherical and cylindrical expansions with the DSMC method, Bird found that breakdown of translational equilibrium occurred when P exceeded 0.05. Bird also showed that this parameter can be used to estimate the breakdown of rotational equilibrium. However, the simulation methods

used a constant rotational collision number of 2, which under predicts the rotational relaxation process for typical gases [25].

$$P = \frac{1}{\nu}\left|\frac{D\left(\ln\rho\right)}{Dt}\right| \tag{2}$$

Boyd et al. [26, 27] have proposed a gradient-length Knudsen number, shown in Eq. 3 where λ is the local mean free path and Q is some macroscopic flow quantity of interest, such as density, flow speed, or temperature.

$$Kn_{\mathrm{GL-Q}} = \lambda\left|\frac{\nabla Q}{Q}\right| \tag{3}$$

The local mean free path used in the gradient-length Knudsen number is calculated using Eq. 4 where n is the number density, T_{TRA} is the translational temperature, ω is the macroscopic viscosity temperature exponent, and T_{ref} is the temperature that the reference cross section, σ_{ref}, is calculated at, which is consistent with the variable hard sphere collision model [1] used in the DSMC simulation and the corresponding temperature viscosity relation used within the CFD module. The reference cross section can be calculated using Eq. 5 where k is the Boltzmann constant and μ_{ref} is the coefficient of viscosity at T_{ref}.

$$\lambda = \frac{1}{\sqrt{2}n\sigma_{ref}}\left(\frac{T_{\mathrm{TRA}}}{T_{ref}}\right)^{\omega-1/2} \tag{4}$$

$$\sigma_{ref} = \frac{15\sqrt{\pi m k T_{ref}}}{2\left(5-2\omega\right)\left(7-2\omega\right)\mu_{ref}} \tag{5}$$

The gradient-length Knudsen numbers are directly related to the Chapman-Enskog expansion terms for mass, momentum, and energy molecular diffusion. Through detailed comparison of kinetic and continuum simulations of planar shock waves, spherically blunted bodies, and interaction flows, Boyd et al. found that in regions where the maximum gradient-length Knudsen number exceeded 0.05, the difference between full DSMC and full CFD exceeds 5%. Therefore, a conservative breakdown parameter of 0.05, such that DSMC is used when $\max\left(Kn_{\mathrm{GL-Q}}\right) > 0.05$ and CFD is used elsewhere, should not introduce more than 5% error within a hybrid method. Recent results [28, 29] with a hybrid DSMC-CFD method have shown that relaxing the breakdown parameter to a value of 0.1 still produces hybrid predictions that remain in excellent agreement with full DSMC simulation results.

Similarly, Garcia et al. [30] have proposed a breakdown parameter based directly on the expansion terms of the Chapman-Enskog distribution function, which is shown in Eq. 6 and where the normalized shear stress and heat flux terms are shown in Eqs. 7 and 8, respectively. A conservative switching criterion of 0.1, such that DSMC is used when $B > 0.1$ and CFD is used otherwise, has been proposed [31] while in practice, the switching criteria has been successfully relaxed to 0.2 for certain flows [32].

$$B = \max\left(\left|\tau^*_{i,j}\right|, \left|q^*_i\right|\right) \tag{6}$$

$$\tau^*_{i,j} = \frac{\mu}{p}\left(\frac{\partial u_i}{\partial x_j} + \frac{\partial u_j}{\partial x_i} - \frac{2}{3}\frac{\partial u_k}{\partial x_k}\delta_{i,j}\right) \tag{7}$$

$$q^*_i = -\frac{\kappa}{p}\sqrt{\frac{2m}{kT}}\frac{\partial T}{\partial x_i} \tag{8}$$

Tiwari [33] has proposed a switching criteria, $\|\phi\|$, as shown in Eq. 9 where q is the heat flux vector, τ is the shear stress tensor, ρ is the local mass density, R is the universal gas constant, and T is the local translational temperature. For the continuum approximation to hold, Tiwari reasoned that this parameter must be much less than unity, therefore Tiwari stated that kinetic solvers should be used anywhere that $\|\phi\| > \epsilon$, where ϵ is much less than unity.

$$\|\phi\| = \frac{1}{\rho RT}\left[\frac{2}{5}\frac{|q|^2}{RT} + \frac{1}{2}\|\tau\|^2\right]^{1/2} \tag{9}$$

Recently, Lockerby et al. [34] have proposed a switching criterion, shown in Eq. 10, that compares the difference between typical shear stress and heat flux terms used to close the Navier-Stokes equations (Newtonian fluid and Fourier's Law) and the third order physically accurate Regularized 13-Moment (R13) equations [35]. They have also formulated an estimate of the R13 shear stress and heat flux terms using only information available from the Navier-Stokes equations so that the breakdown parameter can be calculated without a full R13 solution.

$$Kn_\tau = \frac{\left\|\tau_{i,j}^{(\mathrm{R13})} - \tau_{i,j}^{(\mathrm{NS})}\right\|}{\left\|\tau_{i,j}^{(\mathrm{NS})}\right\|}, \quad Kn_q \frac{\left\|q_i^{(\mathrm{R13})} - q_i^{(\mathrm{NS})}\right\|}{\left\|q_i^{(\mathrm{NS})}\right\|} \tag{10}$$

In addition to collisional nonequilibrium, a hybrid method must ensure that DSMC is used in other regions of the flow where certain physical processes, such as rotational relaxation, are important but are ignored in the continuum module. For example, if the continuum module assumes that translational and rotational modes are in equilibrium, then the hybrid method should ensure that regions that can be considered in collisional equilibrium, such that the velocity distribution function can be described by a Chapman-Enskog velocity distribution function, but where the rotational mode is not in equilibrium with the translational mode be assigned to the DSMC module. For near equilibrium flows over blunt bodies, which are of interest for hybrid methods, almost the entire region behind the strong expansion displays significant nonequilibrium between the rotational and translational energy modes. This would greatly increase the size of the region simulated with the DSMC module in a hybrid simulation and have a serious adverse effect on the numerical efficiency. Schwartzentruber et al. [36, 28, 37] found that only the strong thermal relaxation behind a strong bow shock had a large adverse effect on the physical accuracy of the hybrid method and proposed an additional breakdown parameter shown in Eq. 11 with a switching parameter of 0.01 so that regions where the translational temperature exceeds the rotational temperature by more than 1% are simulated with the DSMC method.

$$Kn_{\mathrm{ROT-NEQ}} = \frac{(T_{\mathrm{TRA}} - T_{\mathrm{ROT}})}{T_{\mathrm{ROT}}} \tag{11}$$

In addition to the strong bow shock, this additional breakdown parameter has been found to increase the size of the DSMC region behind the recompression wave in the wake of blunt body flows [38]. This has an adverse effect on the efficiency of a hybrid method, but is required to maintain sufficient physical accuracy. By inclusion of a separate rotational energy equation in the continuum module, nearly the entire region that displays rotational nonequilibrium with near translational equilibrium can be instead simulated within the continuum module with little physical error.

However, even if a separate rotational energy equation is included in the continuum module, the additional breakdown parameter is still needed to ensure the the rotational energy probability density function is near

equilibrium in the continuum region, but the breakdown value can be relaxed to 0.1 such that DSMC is used in all regions where the rotational temperature deviates from the translational temperature by more than 10%.

For example, Fig. 13 shows a comparison of translational temperature prediction of a hybrid method with (top) and without (bottom) the rotational nonequilibrium switch activated along with full DSMC simulation results. Without the nonequilibrium switch, the interface location between the CFD and DSMC modules is located very near the shock. Since CFD does not contain the physical accuracy required to model this portion of the rotational relaxation process as the rotational energy distribution function is highly non-Boltzmann in this region, the post shock temperatures are over predicted compared to full DSMC. With a rotational nonequilibrium cutoff parameter of 0.1, such that DSMC is used in regions where the difference between the translational and rotational temperatures exceeds 10% of the rotational temperature, the portion of the flow field modeled with the continuum solver is slightly decreased to only regions where the continuum solver is physically valid and agreement between the hybrid method and full DSMC results is greatly improved.

In addition, velocity and rotational energy distribution functions are sampled from the full DSMC solution at locations at the edge of the interface location predicted by each of the hybrid simulations denoted as **A** and **B** in Fig. 13. Figures 14a and 14b, respectively, compare the velocity distribution functions and rotational energy distribution function sampled at point **A** from DSMC with equilibrium theory. Although the velocity probability density functions are in excellent agreement with equilibrium theory, the rotational energy distribution function differs significantly from equilibrium. The peak in the rotational energy probability density function at low rotational energies signifies that there is still a large number of particles that have not experienced a rotationally inelastic collision at the post shock temperature and still maintain the slope of an equilibrium probability density function at the free stream temperature. In contrast, Figs. 15a and 15b compare the velocity and rotational energy distribution functions, respectively, at the continuum interface location computed with the added breakdown parameter at point **B**. At this point in the flow, both the velocity *and* rotational energy probability density functions are in much better agreement with the equilibrium description and the models used in the continuum solver are valid. Since the equilibrium rotational energy distribution function is calculated based on the average rotational energy, comparison of higher order moments, such as the variance, calculated from sampled data and the equilibrium distribution can be used as a measure of degree of rotational nonequilibrium. At point **A**, the sampled variance differs by nearly 25% from equilibrium, while the sampled variance differs by less than 10% from the equilibrium value at point **B**.

3.2 Coupling Procedures

The method of information transfer between particle and continuum methods can typically be split into two categories: coupling by maintaining consistent fluxes or coupling by maintaining consistent state properties in reservoir cells. Figure 16 provides a visual comparison of the two coupling methods. A flux-based, coupling method, which is depicted in Fig. 16(a), involves calculating fluxes of conserved variables at the interface location according to particle cell, F_{P}, and according to the continuum cell, F_{C}. The particle flux can be directly calculated by tracking the number of particles that cross the interface, but the continuum flux must be extrapolated using macroscopic cell-averaged state quantities and their gradients. In general, the estimated fluxes are not the same and are often modified to ensure that mass, momentum, and energy are conserved within the simulation. This modified flux is applied as a boundary condition to both simulation techniques and is used to update the

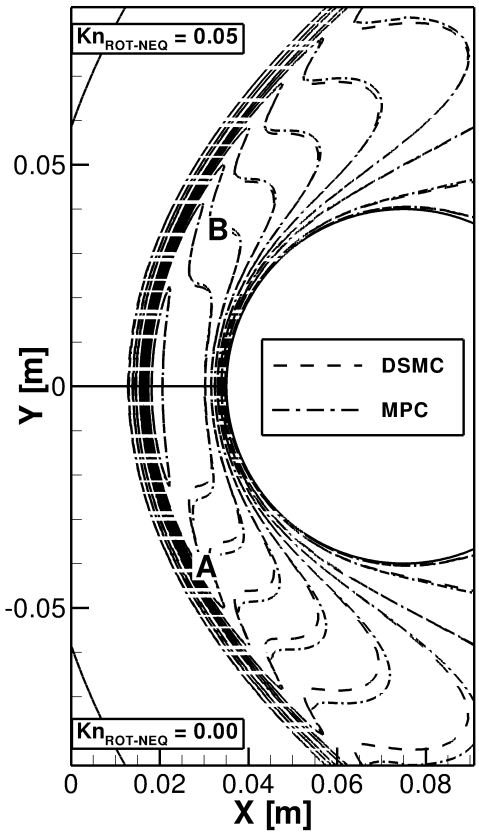

Figure 13: Comparison of translational temperatures predicted by the MPC method with (top) and without (bottom) the rotational nonequilibrium breakdown parameter compared with full DSMC of Mach 12 flow over a cylinder with a global Knudsen number of 0.01 [38]

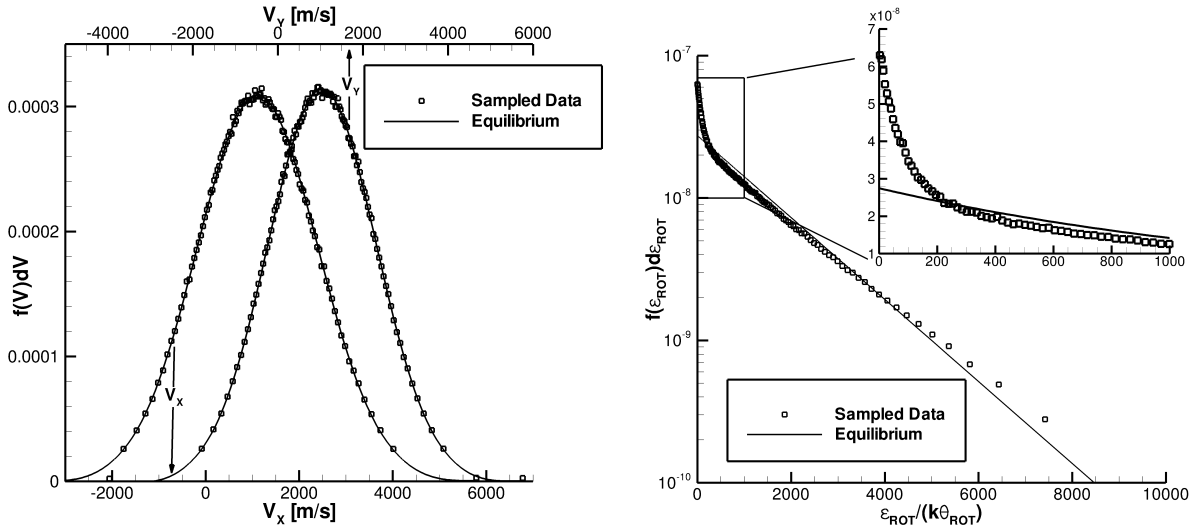

(a) Velocity probability density functions

(b) Rotational energy probability density function

Figure 14: Comparison of probability density functions predicted by DSMC and equilibrium theory at point **A** shown in Figure 13 [38]

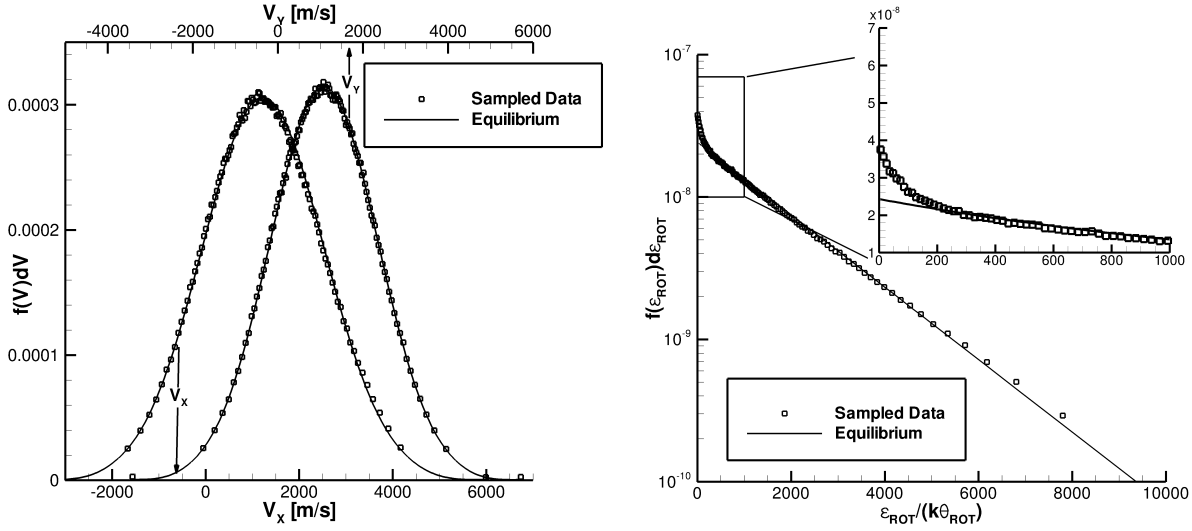

(a) Velocity probability density functions

(b) Rotational energy probability density function

Figure 15: Comparison of probability density functions predicted by DSMC and equilibrium theory at point **B** shown in Figure 13 [38]

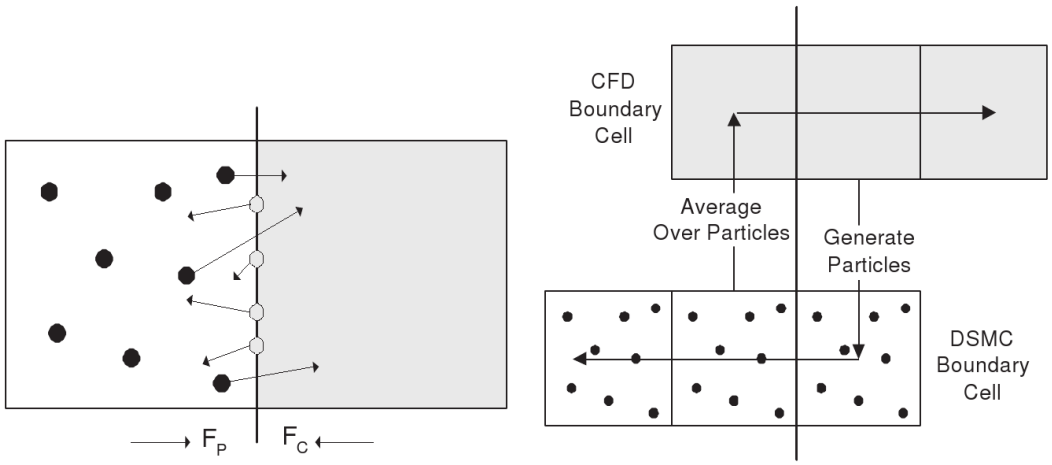

(a) Flux-based coupling. (b) State-based coupling.

Figure 16: Schematic of typical hybrid coupling procedures

continuum solution and to estimate the probability density functions that are sampled to assign DSMC particle information.

With state-based coupling, shown in Fig. 16(b), transfer of information between simulation methods is performed by one method providing a Dirichlet boundary condition to the other simulation technique. Each method can then update its respective regions using algorithms internal to the corresponding simulation method. For coupling from the particle to the continuum method, these values are calculated by performing an averaging procedure to sample state quantities of interest, such as average density, velocity, and energy in DSMC cells along the edge of the interface location. These values are assigned to continuum ghost cells which are used to calculate inviscid and viscous fluxes to update the solution within the continuum domain. For coupling from the continuum to the particle method, average state and gradient information is used to estimate the probability density functions in DSMC boundary cells. Before each particle iteration, all simulators in these boundary cells are deleted and new particles are generated consistent with the estimated probability density functions constructed from the continuum data. Then, simulators in reservoir cells are allowed to move throughout the domain using the internal DSMC move algorithm.

For both coupling procedures, techniques to reduce the statistical scatter are often employed to ensure that the continuum method remains stable. For many flows that involve strong two-way coupling, the efficiency of the hybrid method is determined by how often information is passed between flow modules. Unfortunately, the statistical scatter of averaged DSMC data over very few time-steps can have large variations at the continuum-rarefied boundary that could create numerical instabilities in the continuum module. Many techniques to reduce this statistical scatter have been proposed for different hybrid methods and will be reviewed in the following subsection.

Often, an overlap region between the continuum and particle boundary cells is also used, where the particle region is extended into the continuum domain and both simulation methods calculate the solution. These overlap cells can be used to filter the physical inaccuracies from an incorrect initial solution or to compare simulation

predictions to ensure that the interface location is located in a near continuum region, where the Navier-Stokes equations are appropriate.

4 Hybrid Codes and Their Application

Over the past two decades, many studies of hybrid particle-continuum techniques have been performed that have continuously expanded the state of the art capabilities.

Wadsworth and Erwin developed a strongly coupled, flux-based hybrid DSMC-CFD scheme and applied it both to simulate one dimensional shocks [39] and two dimensional rarefied slit flow [40]. In these studies, a Maxwellian distribution was used to generate simulation particles at the interface location, which was consistent with the governing Euler equations in the continuum region while the domain boundaries remained fixed. Although the flow was unsteady, the scheme used cumulative averages to calculate the particle to continuum flux to reduce the inherent statistical scatter, while the continuum to particle flux was time accurate based on the current continuum solution.

Hash and Hassan also coupled particle and continuum codes using a flux-based procedure to simulate Couette flow [41] and near equilibrium, hypersonic flow over a sting-mounted blunted sphere-cone [42, 43]. Bird's DSMC method that took into account internal excitation and finite rate chemistry was used as the DSMC module while the modified Navier-Stokes equations were solved on a structured grid in the continuum module. Both the Marshak condition and property interpolation technique were employed to transfer information at the interface. Along much of the rarefied-continuum interface location for the hypersonic flow case, the normal Mach number was small which greatly increased the statistical scatter associated with particle fluxes at the boundary. The statistical scatter was reduced using a smoothing operator over highly sampled data for the property extrapolation before imposing the flux boundary condition. Although these smoothing procedures reduced the scatter for bulk properties, oscillations of properties with large gradients along the boundary could produce unphysical, negative values of density. In addition, the statistical scatter of gradients were still appreciable with low order smoothing operators so a fourth-order smoothing procedure with a 7-point stencil had to be used in certain regions. To maintain consistency at the interface, the researchers also found that sampling particle velocities from the Chapman-Enskog velocity probability density function was necessary in regions that displayed significant momentum or energy transfer [41].

Roveda et al. proposed a hybrid particle-continuum method that used a state-based coupling procedure to simulate moving planar shock waves [44] and two dimensional unsteady flow [45]. The continuum module solved the Euler equations using Nadiga's adaptive discrete velocity (ADV) method [46], while Bird's DSMC method was used in the particle module. Although the state-based procedure had less statistical scatter at the boundary when compared to flux-based coupling procedures, the method was time-accurate which reduced the number of statistically independent samples to the current number of DSMC simulator particles in each cell. In order to reduce the statistical scatter in boundary cells, their method used a novel algorithm to clone particles in a buffer around the rarefied region to increase the number of nearly statistically independent DSMC samples. This had an effect of reducing the statistical scatter by over a factor of two. Two layers of DSMC reservoir cells were constructed along the DSMC boundary and particles were assigned velocities from the Maxwell-Boltzmann velocity distribution function which is consistent with the continuum solver used in this work.

Garcia et al. proposed an adaptive mesh and algorithm refinement method [31, 32] that introduces the DSMC methodology at the highest level of refinement of an adaptive mesh scheme. During each time-step, the continuum method is applied to the entire flow. Then, regions that are labeled as nonequilibrium regions are resolved with a finer mesh that meets DSMC requirements and multiple DSMC time-steps are taken to match the larger, continuum time-step. Particles are generated in reservoir cells around DSMC regions consistent with the time-interpolated continuum data, while particle fluxes across each continuum face are recorded. After the DSMC simulation procedure has reached the current continuum time, DSMC samples are used to update the applicable continuum cells and conserved fluxes are calculated based on the sampled particle simulator fluxes. This method has been successfully applied to one- and two-dimensional gas flows.

Sun et al. [47] have proposed a hybrid method that couples a Navier-Stokes solver with a novel information preservation (DSMC-IP) method to simulate micro-scale flows. The IP method is an extension of Bird's DSMC method that tracks additional macroscopic variables in each DSMC cell that contain less statistical scatter. The reduced statistical scatter of the IP method allows it to be tightly coupled with a Navier-Stokes solver with little effect on the stability in continuum regions. They found that Garcia's breakdown parameter [30, 31] worked best for near equilibrium, micro-scale gas flows. Figure 17 shows a schematic of the state-based coupling procedure at the continuum-rarefied interface location. Reservoir cells are used and particle velocities are assigned by sampling the Chapman-Enskog velocity distribution function using the continuum information in the corresponding cells. Application of the NS/DSMC-IP hybrid method has been successful on many micro-scale flows including Couette flow, Rayleigh flow, and external flow over micro-airfoils. For example, Fig. 18 shows a comparison of flow velocity around a flat plate at zero angle of attack predicted by full Navier-Stokes, full DSMC-IP, and hybrid NS/DSMC-IP. The hybrid method has been able to successfully reproduce microscopic effects in the rarefied, near-body region that the continuum, Navier-Stokes equations are unable to capture, and has been used to characterize external flow over micro-plates at various angles of attack and Reynolds numbers. For example, Fig. 19 shows a hybrid NS/DSMC-IP prediction of flow over a flat plate with 5% thickness at a 20° angle of attack. Here the rarefied region, which is highlighted in Fig. 20, is confined to a small region near the leading edge. Rather than simulate the entire flow with a rarefied flow method, this hybrid method is able to apply the DSMC-IP method to only regions that exhibit translational nonequilibrium effects.

Wang and Boyd [48] have proposed using the DSMC-IP method coupled to a Navier-Stokes solver within a hybrid framework to simulate partially rarefied, hypersonic flow. Although the method was successful for certain two-dimensional flows, it was found that the DSMC-IP scheme produced an incorrect post-shock state and shock wave thickness when applied to planar shock waves. A new formulation for the DSMC-IP energy flux [49] provided a partial remedy to the discrepancies, but at a large computational expense. The hybrid NS/DSMC-IP method has been applied to planar shock waves, a blunted cone with a small nose radius, and the hollow cylinder-flare experimental case that was described in the viscous interaction flow subsection.

Wu et al. [50] have proposed a parallel coupled DSMC-NS method to simulate hypersonic flow over a 25° wedge and expansion of nitrogen gas from a three-dimensional nozzle into a near-vacuum container. The authors used a shell script that coupled existing DSMC and CFD codes. State-based coupling was used to transfer information between the two simulation methods. The DSMC region is extended into the continuum region and the breakdown parameter is continuously applied to the flow field to ensure that the interface location remains in a continuum location. Though the continuum method solved the Navier-Stokes equations, the particles generated at the continuum-rarefied interface were assigned velocities consistent with the Maxwell-Boltzmann

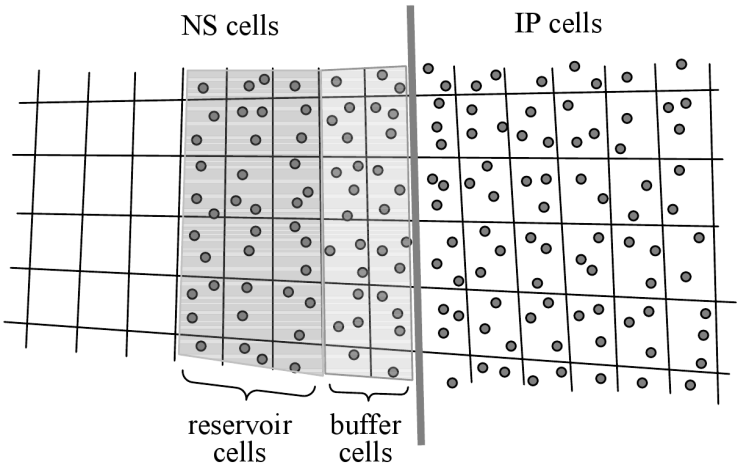

Figure 17: Schematic of DSMC-IP/NS coupling [47]

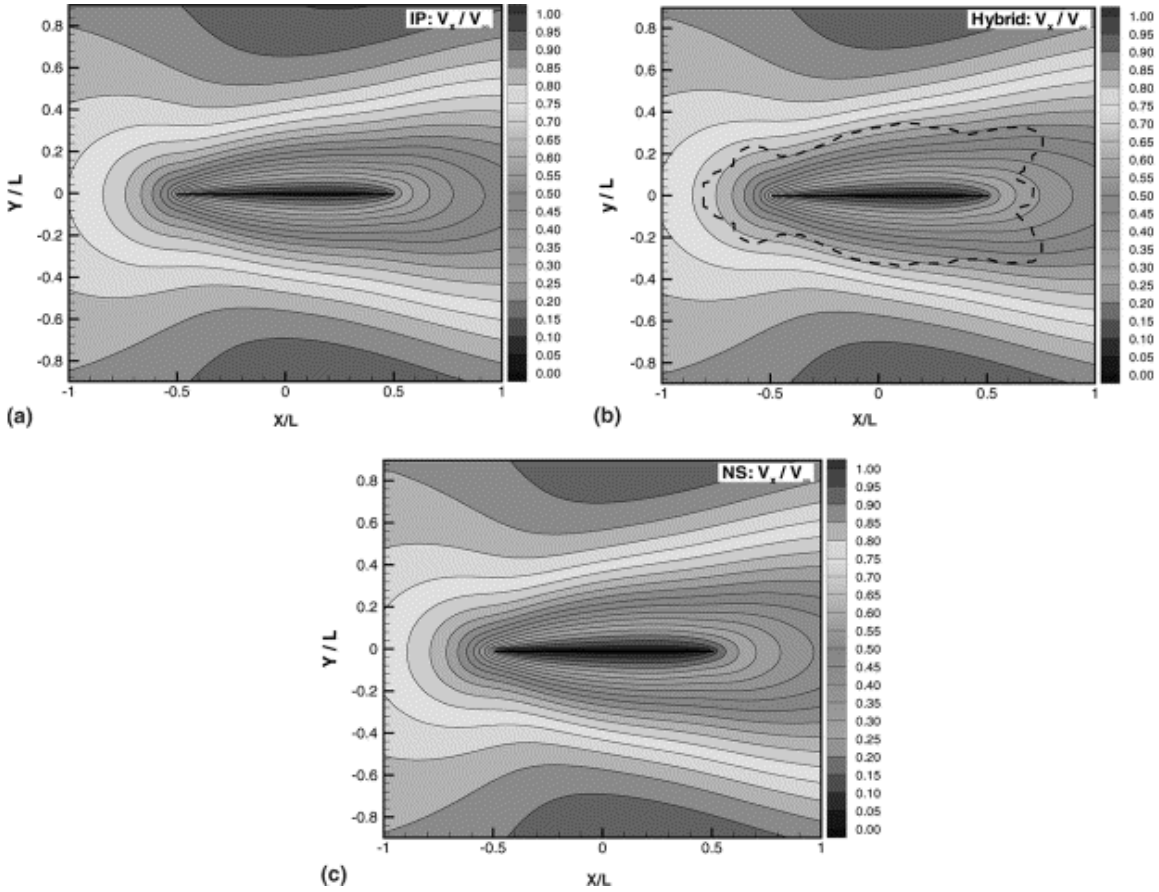

Figure 18: Prediction of micro-scale flow over a flat plate with DSMC-IP, Navier-Stokes solver, and hybrid DSMC-IP/NS [47]

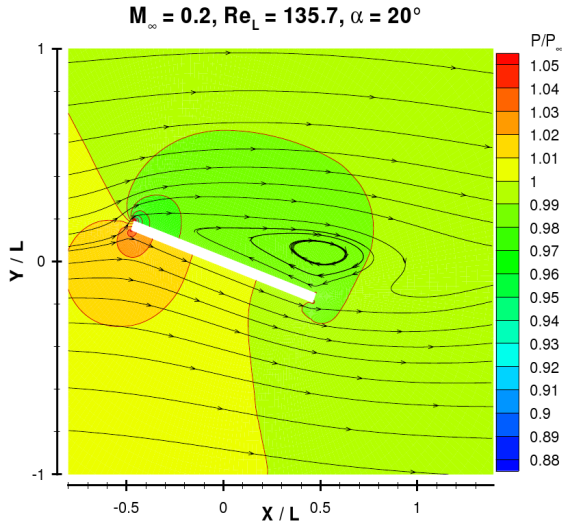

Figure 19: Prediction of Mach 0.2 flow over a flat plate at a 20° angle of attack with hybrid DSMC-IP/NS [47]

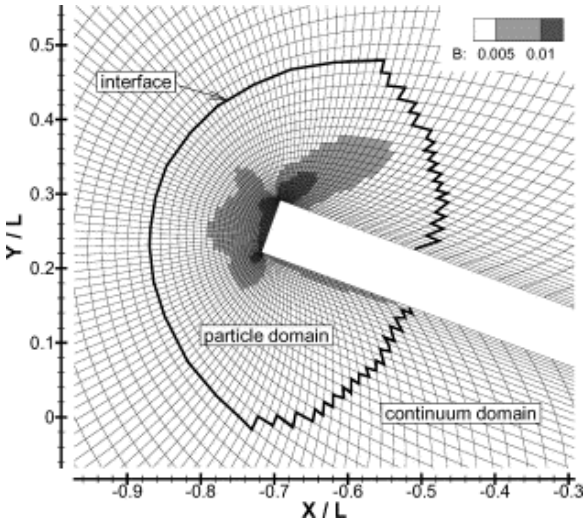

Figure 20: Enlargement of the continuum/rarefied demarcation near the leading edge of Mach 0.2 flow over a flat plate at a 20° angle of attack [47]

velocity distribution function to increase efficiency. Initially, the hybrid method used the maximum gradient length Knudsen number with a cutoff parameter of 0.02 to ensure that the interface location was in a region that was very near equilibrium. However, when compared to a full DSMC simulation, the hybrid simulation took about 20% more computational time. The continuum code used a single temperature to describe the translational and rotational modes which required an additional thermal breakdown parameter very similar to that shown in Eq. 11 to ensure that regions that displayed rotational nonequilibrium effects are simulated with the DSMC method. To improve the efficiency, later work [51] used only the gradient length Knudsen number based on pressure which then includes most of the boundary layer to be simulated with the continuum method instead of the DSMC module. The cutoff parameter was also relaxed to a value of 0.05. In addition, the rotational breakdown parameter was reformulated to Eq. 12 where T_q is the temperature associated with the qth energy mode, ζ_r is the number of rotational degrees of freedom, and ζ_v is the number of vibrational degrees of freedom. A cutoff parameter value of 0.03 was employed for this additional switch such that DSMC is used in regions where $P^*_{The} > 0.03$.

$$P^*_{The} = \sqrt{\frac{\left(\frac{T_x}{T_{tot}} - 1\right)^2 + \left(\frac{T_y}{T_{tot}} - 1\right)^2 + \left(\frac{T_z}{T_{tot}} - 1\right)^2 + \zeta_r \left(\frac{T_r}{T_{tot}} - 1\right)^2 + \zeta_v \left(\frac{T_v}{T_{tot}} - 1\right)^2}{3 + \zeta_r + \zeta_v}} \tag{12}$$

The number of coupling iterations was also reduced from six to four which resulted in the hybrid method requiring nearly a factor of 2 less computational time compared to the corresponding full DSMC simulation.

Schwartzentruber and Boyd [52] have proposed a Modular Particle-Continuum (MPC) method to simulate partially rarefied, steady-state flow over hypersonic vehicles. This method couples existing DSMC and CFD modules that remain nearly unmodified. State-based coupling is performed with particle velocities assigned by sampling of the Chapman-Enskog velocity distribution function using the algorithm of Garcia and Alder [30], while the statistical scatter of particle samples is reduced by use of a novel subrelaxation scheme of Sun and Boyd [53] which is shown in Eq. 13 where Q is a quantity of interest, j is the current iteration, and Φ is the subrelaxation parameter. Typically a subrelaxation parameter value of 0.001 is used.

$$\langle Q \rangle_j = (1 - \Phi) \langle Q \rangle_{j-1} + \Phi Q_j \tag{13}$$

The method has been successfully applied to reproduce full DSMC predictions for planar shock waves [52], two-dimensional blunt body flows [54, 36] and axi-symmetric blunt body [28] and viscous interaction flows [23]. Though the overall hybrid cycle is similar to that proposed by Wu et al., there is one subtle and important difference. The MPC method does not call the continuum solver until the interface has stopped moving to ensure that the continuum method is applied only in regions where the Navier-Stokes equations are valid. This is vital for the proper simulation of the shock layers over hypersonic, blunt bodies to correctly predict the post-shock condition and shock standoff distance [55].

Recently, extensions of the MPC method have allowed for simulation of rotational [38] and vibrational nonequilibrium [56] throughout the entire flow domain, and the method has been parallelized [57] for distributed memory systems using dynamic domain decomposition routines. The computational speed-up of the MPC method over full DSMC has ranged from about 1.5 for flows that are nearly entirely rarefied to over a factor of 30 for near equilibrium flows.

Although the sub relaxation technique reduces the scatter of macroscopic flow variables, it should only be used if the flow variables of interest are resolved in less than $\frac{1}{\Phi}$ iterations. For almost all flow variables, this can often be done in very few iterations. For vibrational energies, a discrete probability density function is used that is consistent with the simple harmonic oscillator assumption and the number of iterations required to resolve a low vibrational temperature becomes enormous. Figure 21 compares the subrelaxation average rotational and vibrational temperatures as a function of iteration number with 20 particles per iteration at various values of temperature. In general, the rotational temperature (and also translational temperature that is not shown) can be resolved in very few iterations and a subrelaxation parameter of 0.001 is sufficient regardless of the mean energy content since the discrete energy steps of these modes are much less than the mean particle energy content and the energy probability density functions can be considered continuous. In contrast, most free stream vibrational energies are much less than the discrete energy step size and the probability of experiencing a vibrationally excited molecule is extremely low. For example, when the vibrational temperature is less than $0.1\theta_{\text{VIB}}$ (which corresponds to a free stream temperature of less than 339.5 K for N_2), less than two vibrationally excited molecules are found in each set of $\frac{1}{\Phi}$ iterations. Decreasing the subrelaxation parameter, Φ, could decrease the statistical scatter of the subrelaxation averaged vibrational temperature at the expense of efficiency, but typical high altitude temperatures would require Φ to be many orders of magnitude smaller than what is currently used. This would make any coupled hybrid method using this technique slower than full DSMC.

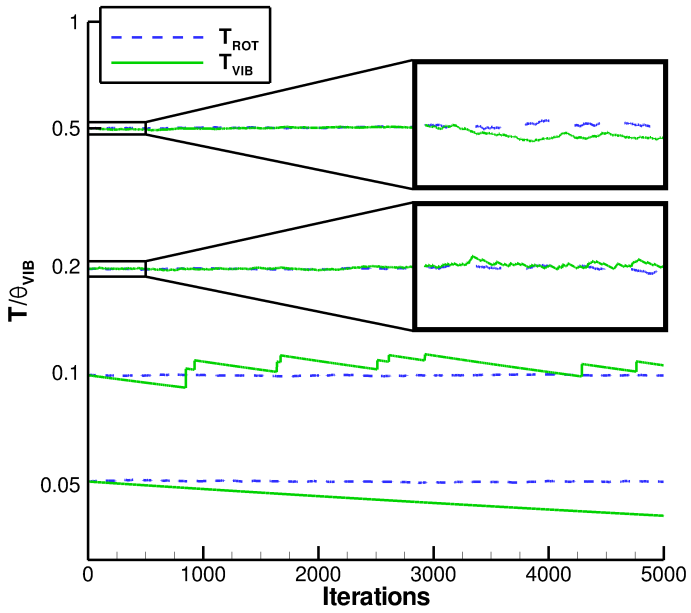

Figure 21: Comparison of the level of statistical scatter of subrelaxation averages of internal temperatures at various levels.

Instead of assigning vibrational energies consistent with the discrete Boltzmann energy probability density function, the average vibrational energy is assigned to all particles in the boundary cells. Equation 14 shows the final calculation of the vibrational energy where N_{max} is the level at which the discrete Boltzmann distribution is

truncated, R is the universal gas constant, ς is the ratio of vibrational temperature to characteristic vibrational temperature shown in Eq. 16, and P_i is the probability of a particle having the ith level of vibrational energy. Assuming vibrational energy is modeled as a simple harmonic oscillator, the probability of a particle being in a vibrational level can be calculated using Eq. 15. The maximum level, N_{max}, is chosen such that the probability of a particle having a vibrational energy greater than that level is less than 1×10^{-8}.

$$E_{\text{VIB}} = \sum_{i=0}^{N_{max}} P_i i \theta_{\text{VIB}} R \tag{14}$$

$$P_i = \exp\left[-i\varsigma\right]\left(1 - \exp\left[-\varsigma\right]\right) \tag{15}$$

$$\varsigma = \frac{T_{\text{VIB}}}{\theta_{\text{VIB}}} \tag{16}$$

At higher vibrational temperatures, such that $\varsigma > 0.2$, vibrational energies can be sampled from the discrete Boltzmann probability density function without adversely affecting the efficiency of the MPC method and may be necessary for physical processes that directly depend on the vibrational energy distribution function such as chemistry. Based on the results shown in Fig. 21, a switching parameter, ς, may be used to change from assigning average energies at low temperatures to sampling energies directly from the discrete Boltzmann energy probability density function at higher temperatures. The current results shown in Fig. 21 suggest that a switching value of 0.5 may be sufficient, such that the average value is assigned when $\varsigma < 0.5$ and particle vibrational energies are sampled from the Boltzmann probability density function when $\varsigma > 0.5$. Regardless of the method used to assign vibrational energies, discrete vibrational levels are selected after vibrationally inelastic collisions.

An example of results obtained by the MPC method for Mach 20 flow over a sting-mounted planetary probe with a global Knudsen number of 0.01 is shown in Figs. 22-27. This flow condition corresponds to a low density experiment performed at the CNRS facility in France [58, 59, 60]. Due to the very low free stream densities associated with this expansion tunnel, the vibrational energy is assumed to be frozen at room temperature for all flow conditions. The variation in mean free path around the probe and initial and final rarefied-continuum interface locations are shown in Fig. 22. Two MPC simulations were applied to this flow condition, one with rotational nonequilibrium only applied in the DSMC method (Rot. Eq.) [28] and one simulation with rotational nonequilibrium modeled through the entire flow region (Rot. Neq.) [29]. Both MPC predictions are compared to full CFD and full DSMC simulation results. Figure 23 compares the rotational temperature contours predicted by the MPC (Rot Neq), full DSMC, and full CFD. In general, the MPC method has improved agreement with full DSMC results over the initial CFD result across the entire flow field. Even in regions where the CFD module is used, the MPC method has obtained improved boundary conditions from the DSMC solver which has allowed the CFD solver to shift its result to provide excellent agreement with full DSMC.

Figure 24 illustrates the prediction of flow field properties made by full DSMC, full CFD, and both MPC simulations along the extraction lines shown in Fig. 22. Vertical lines denote the interface location for the corresponding MPC result. Although both MPC results remain in excellent agreement with DSMC very near the surface along C2, the MPC results with a single temperature modeled within the CFD module can not accurately model the strong thermal nonequilibrium that exists along nearly the entire extraction line. In contrast, the MPC prediction with the ability of modeling a separate rotational temperature within the CFD solver remains in excellent agreement with full DSMC along the entire extraction line. In addition, the DSMC region simulated

using the MPC method with the ability to model rotational nonequilibrium within the CFD solver is smaller due to the less restrictive breakdown parameter. Even though there is an increase in computational cost associated with solving an additional conserved variable in the continuum solver, the reduction in cost of the DSMC module outweighs this increase resulting in a decrease in the total computational cost of the MPC method relative to full DSMC. This has been seen for other flows as well [38].

Figures 25 and 26, respectively, compare velocity and rotational energy probability density functions predicted by full DSMC, full CFD, and the MPC method at point A shown in Fig. 23. Due to the high degree of collisional nonequilibrium within the shock, the CFD velocity distribution function which is generated from gradients and the first order Chapman-Enskog expansion does not contain sufficient information to correctly generate the velocity distribution function predicted by full DSMC. In contrast, the MPC method is able to remain in very good agreement with DSMC throughout the entire velocity space. Despite the macroscopic rotational temperature predicted by CFD being within 5% of the full DSMC result, the rotational energy distribution function predicted by full CFD is in poor agreement with the DSMC result throughout the entire rotational energy space. Similar to the velocity distribution function, the MPC method remains in excellent agreement with full DSMC results for the rotational energy probability density function.

Figure 27 compares the surface coefficient of heat flux, defined in Eq. 17, predicted by full DSMC, full CFD, and the MPC method with available experimental measurements.

$$C_H = \frac{q}{\frac{1}{2}\rho_\infty U_\infty^3} \tag{17}$$

Along the fore body where the flow is highly collisional, all three methods are in good agreement with each other and the experimental measurements. Despite this highly collisional flow, CFD still slightly over predicts DSMC and MPC results. This is due to the inability to correctly model the Knudsen layer within the CFD solver. As the flow expands around the corner, full CFD over predicts both DSMC and experimental measurements by over an order of magnitude. In contrast, the MPC method remains in good agreement with both the experimental measurements and the full DSMC results. Similarly, the MPC method remains in excellent agreement with full DSMC and experimental measurements along the sting mount, while full CFD over predicts full DSMC along the entire sting mount.

Abbate et al. [61] have proposed a hybrid method very similar to that proposed by both Wu et al. [50] and Schwartzentruber and Boyd [54], but with the capability of simulating unsteady flows. It has been found that the unsteady hybrid method results are in very good agreement with full DSMC simulation results for unsteady shock tube problems, while requiring less than 20% of the full DSMC computational time. This hybrid method has also been applied to unsteady expansions into a very low density tank.

Recently, Kessler et al. [62] have proposed a Coupled Multiscale Multiphysics Method (CM^3) for simulation of internal micro scale flows. Here, the DSMC method is used as a corrector to the momentum and energy transfer terms in rarefied regions. The continuum Navier-Stokes equations are solved throughout the flow field, then in regions identified as being rarefied, DSMC particles are created and assigned velocities consistent with the Chapman-Enskog velocity distribution function. Next, the DSMC particles are allowed to move and collide using standard techniques until the initial distribution function has evolved. Finally, the shear stress tensor and heat flux vectors are updated in regions where DSMC data is available and used in the continuum module.

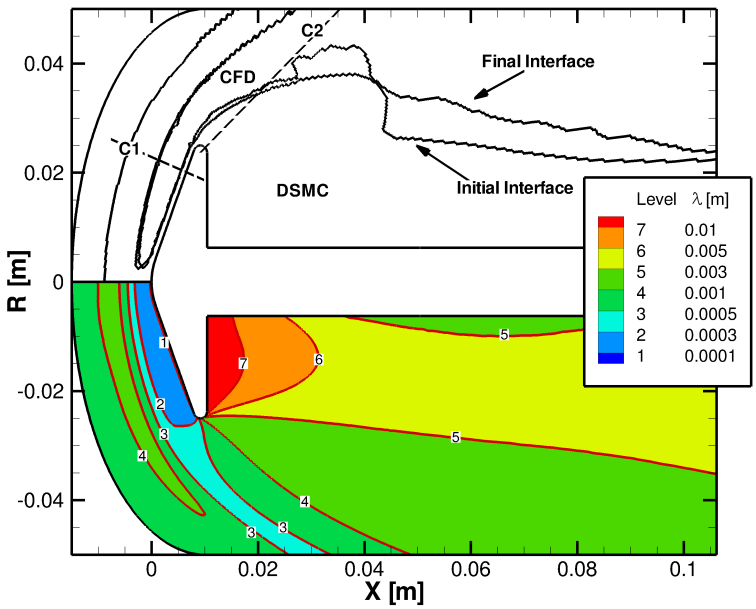

Figure 22: Interface location and variation of mean free path around a hypersonic probe [29]

This process is repeated until the full solution has reached steady state. The CM^3 method has been applied to Couette flow over a range of Knudsen numbers. For example, Fig. 28 shows a schematic of the geometry used to test the CM^3 method, while Fig. 29 shows an example of the simulation results for a Rayleigh flow velocity profile with a global Knudsen number of 0.2 based on the channel height. This flow condition is near the onset of the transition regime where the Navier-Stokes equations with no-slip boundary conditions are not adequate for modeling the flow, but solutions obtained using slip boundary conditions do produce reasonably accurate solutions. With the exception of the very near wall region, the CM^3 method has been successful at matching DSMC and Navier-Stokes with slip predictions. Improvement of the physical accuracy of the CM^3 near walls and increased efficiency are ongoing research topics.

5 Remaining Challenges and Summary

Despite the sophisticated capabilities of hybrid particle-continuum simulation techniques, additional advancements of the technology can still be achieved. One area is further study of a predictor of continuum breakdown. Many of the switching parameter values outlined in Sec. 3.1 have been found by comparison of predictions of fully continuum and kinetic simulation techniques. However, in all flows of interest for application of hybrid particle-continuum methods, the continuum regions are dependent on accurate prediction of nearby rarefied regions. Therefore, full simulations of these flows with a continuum method can shift the results in regions that are truly continuum. Additional study of the rarefied-continuum breakdown and switching parameter using a hybrid particle-continuum simulation technique may result in a more appropriate switching parameter that reduces the

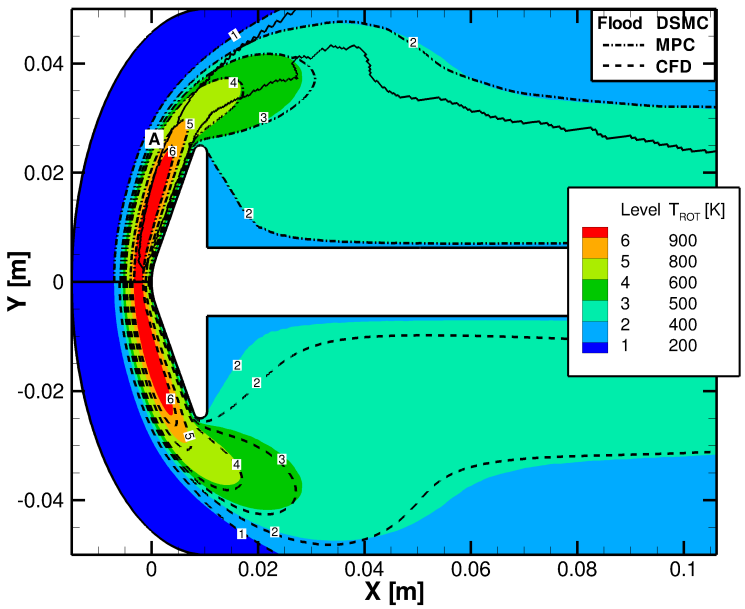

Figure 23: Comparison of translational temperature by DSMC, CFD, and the MPC method [29]

computational cost of hybrid techniques while maintaining the same level of physical accuracy.

Further development of the hybrid methods to simulate full three-dimensional flows may have the largest computational savings over fully kinetic methods. However, very few hybrid particle-continuum methods have demonstrated the capability of simulating these flows over complicated three-dimensional geometries. Further work in this area to mature the technology is still required.

As seen with the inclusion of rotational and vibrational energy nonequilibrium within the MPC method, the use of additional physical models within a hybrid particle-continuum code may require extra considerations to maintain a high level of physical accuracy. Very few studies of the effect of dissociation [63, 64] and ionization on continuum breakdown have been performed. Among other unknown difficulties, the mitigation of the statistical scatter associated with trace species may be necessary.

Hybrid particle-continuum simulation techniques have evolved over the past two decades as a powerful analysis tool for computation of flows that can not be fully simulated with either continuum or kinetic methods and still maintain both physical accuracy *and* numerical efficiency. Typical multi-scale flows that may require application of a hybrid particle-continuum method have been described. A review of demarcation and coupling procedures used to construct hybrid methods has been provided. A review of proposed hybrid particle-continuum methods along with examples of a selection of hybrid simulation results has been given. Finally, a survey of some of the remaining challenges have been described.

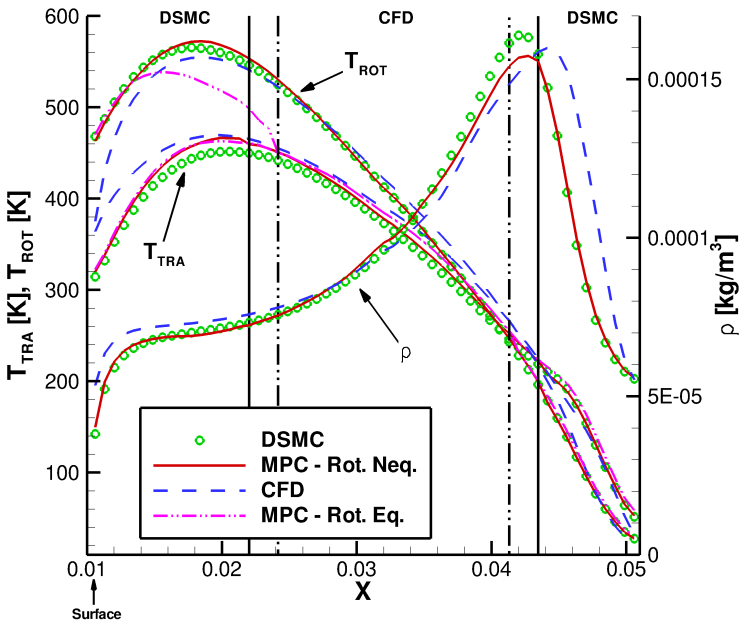

Figure 24: Temperature and density predicted by DSMC, CFD, MPC (Rot. Neq.), and the MPC method (Rot. Eq.) along C2 [29]

6 Acknowledgments

The authors gratefully acknowledge funding provided to support this work by the NASA Aeronautics Research Mission Directorate (grant NNX08AD02A) and the NASA Constallation University Institutes Program (grant NCC3-989).

References

[1] Bird, G. A., *Molecular Gas Dynamics and the Direct Simulation of Gas Flows*, Clarendon Press, 1994.

[2] Wilmoth, R. G., Mitcheltree, R. A., Moss, J. N., and K., D. V., "Zonally Decoupled Direct Simulation Monte Carlo Solutions of Hypersonic Blunt-Body Flows," *Journal of Spacecraft and Rockets*, Vol. 31, No. 6, 1994, pp. 971–979.

[3] McNeely, M., "Microturbine Designed for Mechanical Drive Applications," *Diesel Progress North American Edition*, Vol. 64, No. 5, 1998, pp. 38–40.

[4] Blankinship, S., "New Miniturbine Takes Aim at Microturbine Market," *Power Engineering*, Vol. 105, No. 10, 2001, pp. 77–77.

[5] Lofdahl, L. and Gad-el Hak, M., "MEMS Applications in Turbulence and Flow Control," *Progress in Aerospace Sciences*, Vol. 35, No. 2, 1999, pp. 481–496.

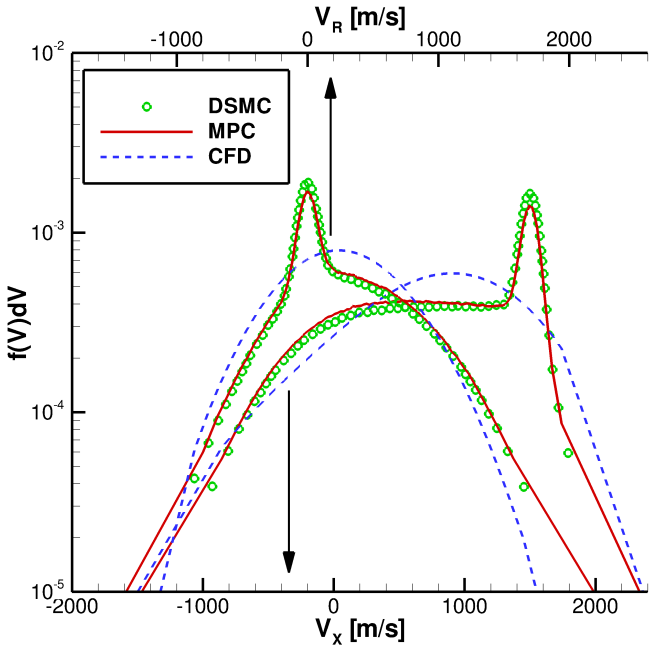

Figure 25: Comparison of velocity distribution functions predicted by DSMC, CFD, and the MPC method within the bow shock [29]

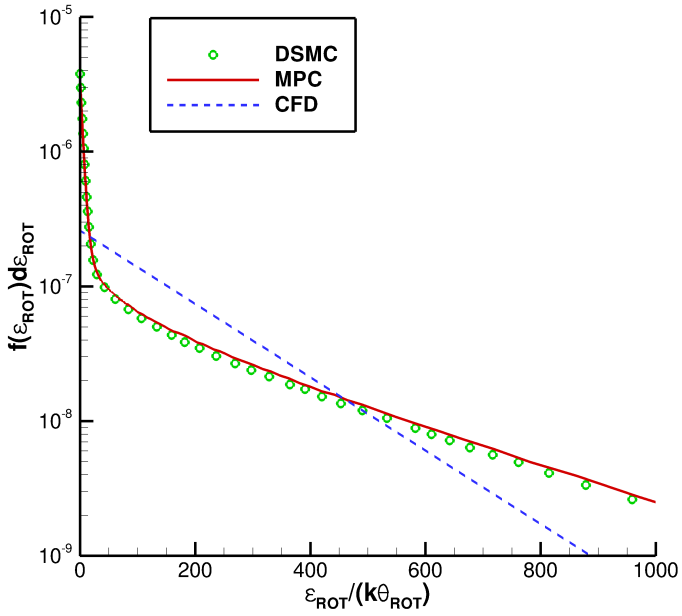

Figure 26: Comparison of rotational energy distribution functions predicted by DSMC, CFD, and the MPC method within the bow shock [29]

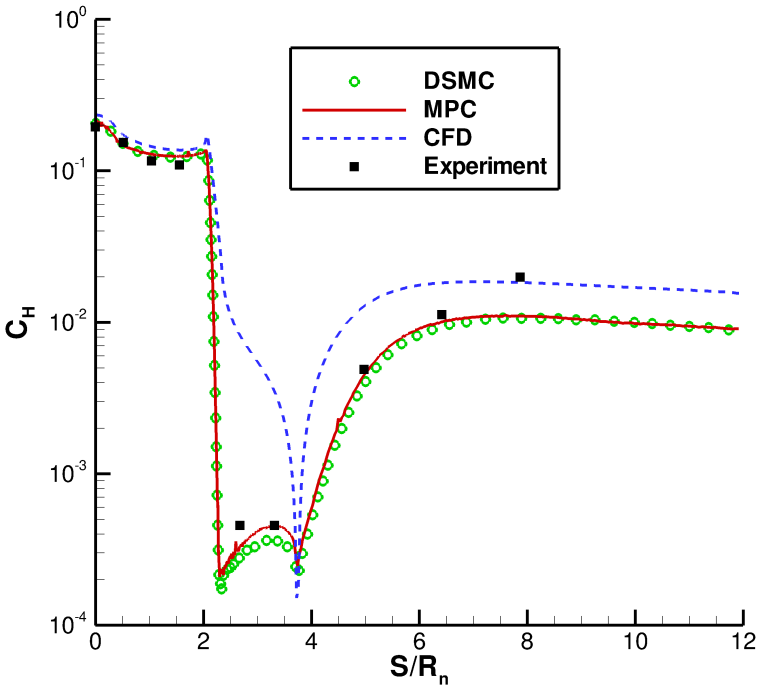

Figure 27: Surface heat transfer along planetary probe [29]

[6] Gad-el Hak, M., "The Fluid Mechanics of Microdevices - The Freeman Scholar Lecture," *Journal of Fluids Engineering*, Vol. 121, 1999, pp. 5–33.

[7] Hagleitner, C., Hierlemann, A., Lange, D., Kummer, A., Kerness, N., Brand, O., and Baltes, H., "Smart Single-Chip Gas Sensor Microsystem," *Nature*, Vol. 414, No. 6861, 2001, pp. 293–296.

[8] Gad-el Hak, M., "Flow Control: The Future," *Journal of Aircraft*, Vol. 38, No. 3, 2001, pp. 402–418.

[9] Rossi, C., Do, C. T., Esteve, D., and Larangot, B., "Fabrication and Modeling of MEME-Based Microthrusters for Space Application," *Smart Materials & Structures*, Vol. 10, No. 6, 2001, pp. 1156–1162.

[10] Pong, K. C., Ho, C. M., Liu, J., and Tai, Y. C., "Non-linear Pressure Distribution in Uniform Microchannels," *Applications of Microfabrication to Fluid Mechanics, ASME Winter Annual Meeting*, Chicago, 1994, pp. 51–56.

[11] Arkilic, E. B., *Measurement of the Mass Flow and Tangential Momentum Accommodation Coefficient in Silicon Micromachined Channels*, Ph.D. thesis, Massachusetts Institute of Technology, 1997.

[12] Putnam, Z. R., Bairstow, S. H., Braun, R. D., and Barton, G. H., "Improving Lunar Return Entry Range Capability Using Enhanced Skip Trajectory Guidance," *Journal of Spacecraft and Rockets*, Vol. 45, No. 2, March 2008, pp. 309–315.

[13] NASA, "http://grin.hq.nasa.gov - GPN-2000-001938," 1957.

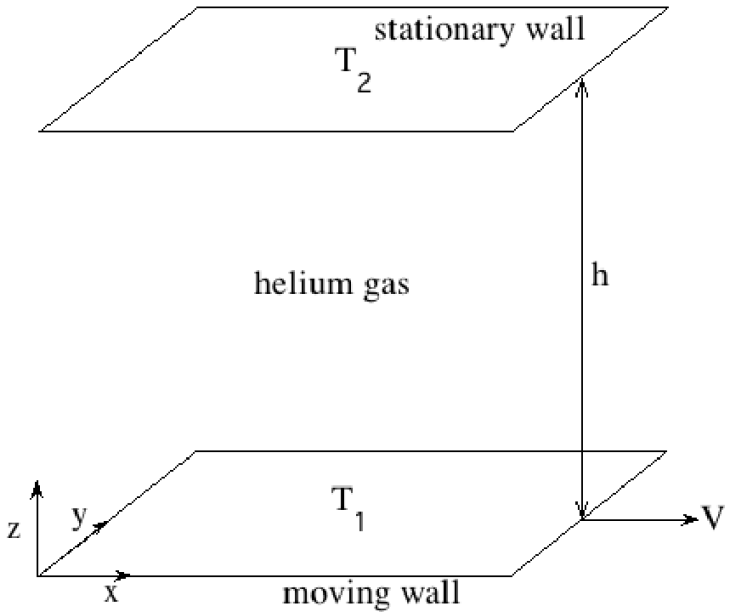

Figure 28: Geometry of the nominally one-dimensional problem used to test CM^3 [62]

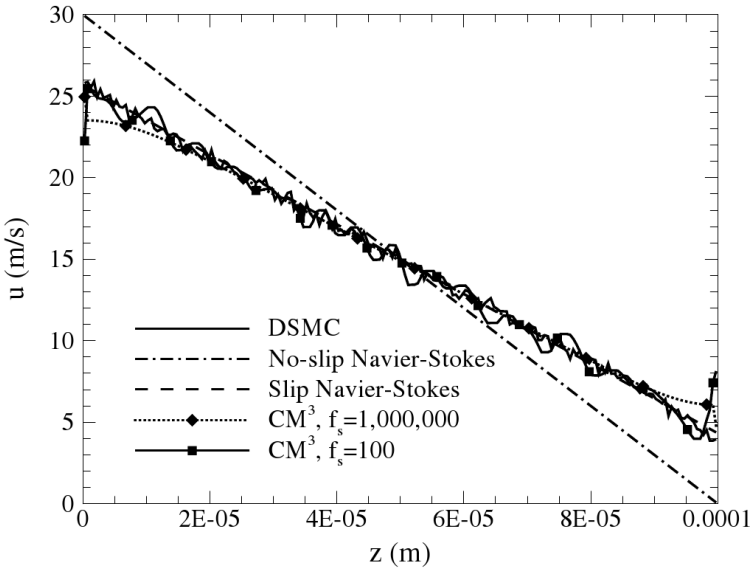

Figure 29: Enlargement of the continuum/rarefied demarcation near the leading edge of Mach 0.2 flow over a flat plate at a 20° angle of attack [62]

[14] Wright, M. J., Prabhu, D. K., and Martinez, E. R., "Analysis of Apollo Command Module Afterbody Heating Part I: AS-202," *Journal of Thermophysics and Heat Transfer*, Vol. 20, 2006, pp. 16–30.

[15] Cianciolo, A. M. D., Davis, J. L., Komar, D. R., Munk, M. M., Samareh, J. A., Williams-byrd, J. A., Zang, T. A., Powell, R. W., Shidner, J. D., Stanley, D. O., Wilhite, A. W., Kinney, D. J., McGuire, M. K., Arnold, J. O., Howard, A. R., Sostaric, R. R., Studak, J. W., Zumwalt, C. H., Llama, E. G., Casoliva, J., Ivanov, M. C., Clark, I., and Sengupta, A., "Entry, Descent, and Landing Systems Analysis Study: Phase 1 Report," 2010.

[16] Clark, I. G., Hutchings, A. L., Tanner, C. L., and Braun, R. D., "Supersonic Inflatable Aerodynamic Decelerators for Use on Future Robotic Missions to Mars," *Journal of Spacecraft and Rockets*, Vol. 46, No. 2, March 2009, pp. 340–352.

[17] Korzun, A. M., Braun, R. D., and Cruz, J. R., "Survey of Supersonic Retropropulsion Technology for Mars Entry, Descent, and Landing," *Journal of Spacecraft and Rockets*, Vol. 46, No. 5, Sept. 2009, pp. 929–937.

[18] Buck, G. M., "Testing of Flexible Ballutes in Hypersonic Wind Tunnels for Planetary Aerocapture," AIAA 2006-1319, 2006.

[19] Burt, J. M. and Boyd, I. D., "Application of a Multiscale Particle Scheme to High Altitude Rocket Exhaust Flows," AIAA 2009-1567, 2009.

[20] Lumpkin III, F. E., Marichalar, J., and Piplica, A., "Plume Impingement to the Lunar Surface: A Challenging Problem for DSMC," June 2007.

[21] Harvey, J. K., Holden, M. S., and Wadhams, T. P., "Code Validation Study of Laminar Shock/Boundary Layer and Shock/Shock Interactions in Hypersonic Flows Part B: Comparison with Navier-Stokes and DSMC Solutions," AIAA 2001-1031, 2001.

[22] Moss, J. N. and Bird, G. A., "Direct Simulation Monte Carlo Simulations of Hypersonic Flows with Shock Interactions," *AIAA Journal*, Vol. 43, No. 12, 2006, pp. 2565–2573.

[23] Schwartzentruber, T. E., Scalabrin, L. C., and Boyd, I. D., "Hyprid Particle-Continuum Simulations of Hypersonic Flow over a Hollow-Cylinder-Flare Geometry," *AIAA Journal*, Vol. 46, No. 8, Aug. 2008, pp. 2086–2095.

[24] Bird, G. a., "Breakdown of translational and rotational equilibrium in gaseous expansions," *AIAA Journal*, Vol. 8, No. 11, Nov. 1970, pp. 1998–2003.

[25] Boyd, I. D., "Analysis of rotational nonequilibrium in standing shock waves of nitrogen," *AIAA Journal*, Vol. 28, No. 11, 1990, pp. 1997–1999.

[26] Boyd, I. D., Chen, G., and Candler, G. V., "Predicting failure of the continuum fluid equations in transitional hypersonic flows," *Phys. Fluids*, Vol. 7, No. 1, Jan. 1995, pp. 210–219.

[27] Wang, W.-L. and Boyd, I. D., "Predicting continuum breakdown in hypersonic viscous flows," *Phys. Fluids*, Vol. 15, No. 1, Jan. 2003, pp. 91–100.

[28] Schwartzentruber, T. E., Scalabrin, L. C., and Boyd, I. D., "Multiscale Particle-Continuum Simulations of Low Knudsen Number Hypersonic Flow Over a Planetary Probe," *Journal of Spacecraft and Rockets*, Vol. 45, No. 6, 2008, pp. 1196–1206.

[29] Deschenes, T. R. and Boyd, I. D., "Application of a Modular Particle-Continuum Method to Partially Rarefied, Hypersonic Flow," *International Symposium on Rarefied Gas Dynamics*, 2010.

[30] Garcia, A. L. and Alder, B. J., "Generation of the Chapman-Enskog Distribution," *Journal of Computational Physics*, Vol. 140, No. 1, Feb. 1998, pp. 66–70.

[31] Garcia, A. L., Bell, J. B., Crutchfield, W. Y., and Alder, B. J., "Adaptive Mesh and Algorithm Refinement Using Direct Simulation Monte Carlo," *Journal of Computational Physics*, Vol. 154, No. 1, Sept. 1999, pp. 134–155.

[32] Wijesinghe, H. S., Hornung, R. D., Garcia, a. L., and Hadjiconstantinou, N. G., "Three-dimensional Hybrid Continuum-Atomistic Simulations For Multiscale Hydrodynamics," *Journal of Fluids Engineering*, Vol. 126, No. 5, 2004, pp. 768.

[33] Tiwari, S., Klar, A., and Hardt, S., "A particle-particle hybrid method for kinetic and continuum equations," *Journal of Computational Physics*, Vol. 228, No. 18, Oct. 2009, pp. 7109–7124.

[34] Lockerby, D. A., Reese, J. M., and Struchtrup, H., "Switching Criteria for Hybrid Rarefied Gas Flow Solvers," *Proceedings of the Royal Society*, Vol. 465, No. 2105, 2009, pp. 1581–1598.

[35] Torrilhon, M., "Regularized 13-moment equations: shock structure calculations and comparison to Burnett models," *International Symposium on Rarefied Gas Dynamics*, Vol. 513, Aug. 2007, pp. 167–172.

[36] Schwartzentruber, T. E., Scalabrin, L. C., and Boyd, I. D., "Hybrid particle-continuum simulations of nonequilibrium hypersonic blunt-body flowfields," *Journal of Thermophysics and Heat Transfer*, Vol. 22, No. 1, 2008, pp. 29–37.

[37] Schwartzentruber, T. E., Scalabrin, L. C., and Boyd, I. D., "Investigation of Continuum Breakdown in Hypersonic Flows using a Hybrid Particle-Continuum Algorithm," AIAA 2008-4108, 2008.

[38] Deschenes, T. R., Holman, T. D., and Boyd, I. D., "Effects of Rotational Energy Relaxation in a Modular Particle-Continuum Method," *Journal of Thermophysics and Heat Transfer, accepted*, 2011.

[39] Wadsworth, D. C. and Erwin, D. A., "One-Dimensional Hybrid Continuum/Particle Simulation Approach for Rarefied Hypersonic Flows," AIAA 90-1690, 1990.

[40] Wadsworth, D. C. and Erwin, D. A., "Two-dimensional hybrid continuum/particle simulation approach for rarefied flows," , No. AIAA paper 1992-2975, 1992.

[41] Hash, D. B. and Hassan, H. A., "Assessment of Schemes for Coupling Monte Carlo and Navier-Stokes Solution Methods," *Journal of Thermophysics and Heat Transfer*, Vol. 10, No. 2, 1996, pp. 242–249.

[42] Hash, D. B., *A Hybrid Direct Simulation Monte Carlo / Navier-Stokes Flow Solver*, Ph.D. thesis, North Carolina State University, 1996.

[43] Hash, D. B. and Hassan, H. A., "Two-Dimensional Coupling Issues of Hybrid DSMC/Navier-Stokes Solvers," AIAA 1997-2507, 1997.

[44] Roveda, R., B., G. D., and Varghese, P. L., "Hybrid Euler/Particle Approach for Continuum/Rarefied Flows," *Journal of Spacecraft and Rockets*, Vol. 35, No. 3, 1998, pp. 258–265.

[45] Roveda, R., B., G. D., and Varghese, P. L., "Hybrid Euler/Direct Simulation Monte Carlo of Unsteady Slit Flow," *Journal of Spacecraft and Rockets*, Vol. 37, No. 6, 2000, pp. 753–760.

[46] Nadiga, B. T. and Pullin, D. I., "A Method for Near-Equilibrium Discrete-Velocity Gas Flows," *Journal of Computational Physics*, Vol. 112, No. 1, 1994, pp. 162–172.

[47] Sun, Q., Boyd, I. D., and Candler, G. V., "A hybrid continuum/particle approach for modeling subsonic, rarefied gas flows," *Journal of Computational Physics*, Vol. 194, No. 1, Feb. 2004, pp. 256–277.

[48] Wang, W. L. and Boyd, I. D., "Hybrid DSMC-CFD Simulations of Hypersonic Flow Over Sharp and Blunted Bodies," AIAA 2003-3644, 2003.

[49] Wang, W.-l. and Boyd, I. D., "A New Energy Flux Model in the DSMC-IP Method for Nonequilibrium Flows," AIAA 2003-3774, 2003.

[50] Wu, J.-S., Lian, Y.-Y., Cheng, G., Koomullil, R. P., and Tseng, K.-C., "Development and verification of a coupled DSMC-NS scheme using unstructured mesh," *Journal of Computational Physics*, Vol. 219, No. 2, Dec. 2006, pp. 579–607.

[51] Lian, Y.-Y., Tseng, K.-C., Chen, Y.-S., Wu, M.-Z., Wu, J.-S., and Cheng, G., "An Improved Parallelized Hybrid DSMC-NS Algorithm," *26th International Symposium on Rarefied Gas Dynamics*, 2009, pp. 341–346.

[52] Schwartzentruber, T. E. and Boyd, I. D., "A hybrid particle-continuum method applied to shock waves," *Journal of Computational Physics*, Vol. 215, No. 2, July 2006, pp. 402–416.

[53] Sun, Q. and Boyd, I. D., "Evaluation of Macroscopic Properties in the Direct Simulation Method," *Journal of Thermophysics and Heat Transfer*, Vol. 19, No. 3, 2005, pp. 329–335.

[54] Schwartzentruber, T. E., Scalabrin, L. C., and Boyd, I. D., "A modular particle-continuum numerical method for hypersonic non-equilibrium gas flows," *Journal of Computational Physics*, Vol. 225, No. 1, July 2007, pp. 1159–1174.

[55] Schwartzentruber, T. E., *A Modular Particle-Continuum Numerical Algorithm for Hypersonic Non-Equilibrium Flows*, Ph.d., University of Michigan, 2007.

[56] Deschenes, T. R., Holman, T. D., Boyd, I. D., and Schwartzentruber, T. E., "Analysis of Internal Energy Transfer Withing a Modular Particle-Continuum Method," AIAA 2009-1213, 2009.

[57] Deschenes, T. R., Holman, T. D., and Boyd, I. D., "Parallelization of Modular Particle-Continuum Method for Hypersonic, Near Equilibrium Flows," Vol. AIAA 2010-, 2010.

[58] Allegre, J., Bisch D., and Lengrand, J. C., "Experimental Rarefied Aerodynamic Forces at Hypersonic Conditions over 70-Degree Blunted Cone," *Journal of Spacecraft and Rockets*, Vol. 34, No. 6, 1997, pp. 719–723.

[59] Allegre, J., Bisch D., and Lengrand, J. C., "Experimental Rarefied Density Flowfields at Hypersonic Conditions over 70-Degree Blunted Cone," *Journal of Spacecraft and Rockets*, Vol. 34, No. 6, 1997, pp. 714–718.

[60] Allegre, J., Bisch D., and Lengrand, J. C., "Experimental Rarefied Heat Transfer at Hypersonic Conditions over 70-Degree Blunted Cone," *Journal of Spacecraft and Rockets*, Vol. 34, No. 6, 1997, pp. 724–728.

[61] Abbate, G., Thijsse, B. J., and Kleijn, C. R., "Coupled Navier-Stokes/DSMC Method for Transient and Steady-State Gas Flows," *Lecture Notes in Computer Science*, Vol. 4487, 2007, pp. 842–849.

[62] Kessler, D. A., Oran, E. S., and Kaplan, C. R., "The Coupled Multiscale Multiphysics Method (CM3) for Rarefied Gas Flows," AIAA 2010-823, 2010.

[63] Holman, T. D., *Numerical Investigation of the Effects of Continuum Breakdown on Hypersonic Vehicle Surface Properties by*, Ph.D. thesis, Unviersity of Michigan, 2010.

[64] Holman, T. D. and Boyd, I. D., "Effects of Continuum Breakdown on Hypersonic Aerothermodynamics for Reacting Flow," *Physics of Fluids*, Vol. Accepted, 2011.